

University of Szeged
Faculty of Pharmacy
Department of Pharmaceutical Chemistry

Enhancing Antibiotic Efficacy through Antimicrobial Peptide-
Mediated Modulation: The Sub-MIC Approach

Ph.D. Thesis

Kaushik Nath Bhaumik

Supervisor:

Prof. Dr. Tamás A. Martinek

Dr. Anasztázia Hetényi

2024

Table of Contents

List of publications and lectures	iii
Abbreviations	v
1. Introduction and goals	1
2. Literature background	3
2.1. Antimicrobial resistance (AMR)	3
2.2. Strategies for countering AMR	3
2.3. Antimicrobial peptides (AMPs)	4
2.3.1. Classification	4
2.3.2. Mechanism of action.....	7
2.3.3. Systems for studying membrane activity.....	12
2.3.4. Advantages of AMPs	13
2.3.5. Sub-MIC activity of AMPs.....	15
3. Experimental methods.....	17
3.1. Synthesis and purification of Peptides	17
3.2. Oxidation of peptides with β -sheet secondary structure.....	17
3.3. Digestion by trypsin and chymotrypsin	18
3.4. Circular Dichroism (CD) Measurements	18
3.5. Preparation of large unilamellar vesicles (LUVs)	18
3.6. NMR measurements.....	19
3.7. Membrane polarisation in LUV model.....	19
4. Results and discussion.....	20
4.1. Designer peptidomimetic foldamers for adjuvant therapy	20
4.1.1. Rational design of PGLa analogues	20
4.1.2. Foldamers synergize with antibiotics.....	23
4.1.3. Foldamers restore antibiotic activity in antibiotic-resistant bacteria.....	23
4.1.4. Foldamer increased survival rate of <i>Galleria mellonella in vivo</i>	24
4.1.5. Foldamers trigger hyperpolarisation of <i>E. coli</i> membrane	25
4.1.6. Foldamers generate diffusion (Goldman-Hodgkin-Katz) potential through selective ion transport.....	27
4.1.7. Stability and toxicity analyses	30
4.2. Assessment of a larger landscape of AMPs for membrane polarisation.....	32
4.2.1. Membrane induced AMP structures hyperpolarise <i>E. coli</i> membrane at sub-MIC....	36

4.2.2.	Concentration-dependent hyperpolarisation by AMPs.....	39
4.2.3.	AMPs generate diffusion potential in LUVs	40
4.2.4.	AMPs transport both cations and anions.....	43
4.3.	Proposed mechanism of hyperpolarisation induced by AMPs.....	44
5.	Conclusion.....	46
6.	Summary	47
	Acknowledgement.....	49
	References	50

List of publications and lectures

Full publications related to thesis

1. **Bhaumik, K. N.**; Hetényi, A.; Olajos, G.; Martins, A.; Spohn, R.; Németh, L.; Jojart, B.; Szili, P.; Dunai, A.; K. Jangir, P.; Daruka, L.; Földesi, I.; Kata, D.; Pál, C.; A. Martinek, T. Rationally Designed Foldameric Adjuvants Enhance Antibiotic Efficacy via Promoting Membrane Hyperpolarization. *Molecular Systems Design & Engineering* **2022**, 7 (1), 21–33.
2. **Bhaumik, K. N.**; Spohn, R.; Dunai, A.; Daruka, L.; Olajos, G.; Zákány, F.; Hetényi, A.; Pál, C.; A. Martinek, T. Chemically diverse antimicrobial peptides induce hyperpolarization of the *E. coli* membrane. *Communications Biology* **2024**, 7, 1-12.

Other full publication

1. Banerjee, S.; Roy, S.; **Bhaumik, K. N.**; Kshetrapal, P.; Pillai, J. Comparative study of oral lipid nanoparticle formulations (LNFs) for chemical stabilization of antitubercular drugs: physicochemical and cellular evaluation. *Artificial Cells, Nanomedicine, and Biotechnology* **2018**, 46, 540–558.
2. Banerjee, S.; Roy, S.; **Bhaumik, K. N.**; Pillai, J. Mechanisms of the effectiveness of lipid nanoparticle formulations loaded with anti-tubercular drugs combinations toward overcoming drug bioavailability in tuberculosis. *Journal of Drug Targeting* **2020**, 28, 55–69.
3. Hetényi, A.; Szabó, E.; Imre, N.; **Bhaumik, K. N.**; Tököli, A.; Füzesi, T.; Hollandi, R.; Horvath, P.; Czibula, Á.; Monostori, É.; Deli, M. A.; Martinek, T. A. α/β -Peptides as Nanomolar Triggers of Lipid Raft-Mediated Endocytosis through GM1 Ganglioside Recognition. *Pharmaceutics* **2022**, 14 (3), 580.

Scientific lectures related to the thesis

1. Bhaumik, K. N.; Hetényi, A.; Olajos, G.; Martins, A.; Spohn, R.; Németh, L.; Jojart, B.; Szili, P.; Dunai, A.; K. Jangir, P.; Daruka, L.; Földesi, I.; Kata, D.; Pál, C.; A. Martinek, T.
Rationally Designed Foldameric Adjuvants Enhance Antibiotic Efficacy via Promoting Membrane Hyperpolarisation.
MTA Peptidkémiai Munkabizottság Ülés (MTA Peptide Chemistry Working Committee Meeting). Balatonszemes, Hungary 2021. October 11-13.
2. Bhaumik, K. N.; Hetényi, A.; Olajos, G.; Martins, A.; Spohn, R.; Németh, L.; Jojart, B.; Szili, P.; Dunai, A.; K. Jangir, P.; Daruka, L.; Földesi, I.; Kata, D.; Pál, C.; A. Martinek, T.
Rationally Designed Foldameric Adjuvants Enhance Antibiotic Efficacy via Promoting Membrane Hyperpolarisation.
10th Interdisciplinary Doctoral Conference. Pécs, Hungary 2021. November 12-13.
3. Bhaumik, K. N.; Hetényi, A.; A. Martinek, T.
Host defense peptides (HDPs) hyperpolarisation membrane by selective ion transport at sub-MIC concentration. (Poster number P038)
Peptide Chemistry and Chemical Biology Symposium
Balatonszemes, Hungary 2022. May 30 – June 1.
4. Bhaumik, K. N.; Hetényi, A.; Olajos, G.; Martins, A.; Spohn, R.; Németh, L.; Jojart, B.; Szili, P.; Dunai, A.; K. Jangir, P.; Daruka, L.; Földesi, I.; Kata, D.; Pál, C.; A. Martinek, T.
Novel foldameric peptide adjuvants counter antimicrobial resistance via promoting membrane hyperpolarisation. (Poster number FP4)
36th European Peptide Symposium and 12th International Peptide Symposium.
Barcelona, Spain 2022. August 28 - September 2.

Abbreviations

AFM: Atomic force microscopy

AMP: Antimicrobial peptide

AMR: Antimicrobial resistance

APD: Antimicrobial peptide database

ATP: Adenosine triphosphate

CCCP: Cyanide-m-chlorophenylhydrazone

CD: Circular dichroism

DCC: N, N'-Dicyclohexylcarbodiimide

DCM: Dichloromethane

DiOC2(3): 3,3'-Diethyloxacarbocyanine Iodide

DiSC2(5): 3,3'-diethylthiadicarbocyanine iodide

DMF: *N,N*-dimethylformamide

DOPC: 1,2-dioleoyl-sn-glycero-3-phosphocholine

DOPG: 1,2-dioleoyl-sn-glycero-3-phospho-(1'-rac-glycerol)

DRAMP: Data repository of antimicrobial peptides

DTT: 1,4-dithiotreitol

E. coli: *Escherichia coli*

EIS: Electrochemical impedance spectroscopy

ESI-MS: Electrospray ionisation mass spectrometry

Fmoc: Fluorenylmethyloxycarbonyl

GHK: Goldman-Hodgkin-Katz

GUVs: Giant unilamellar vesicles

HATU: 1-[bis(dimethylamino)methylene]-1*H*-1,2,3-triazolo[4,5-*b*]-pyridinium-3-oxid hexafluorophosphate

HDP: Host Defense Peptide

HD5: Human α -defensin 5

HEPES: 4-(2-hydroxyethyl)-1-piperazineethanesulfonic acid

HGT: Horizontal gene transfer

HIV: Human immunodeficiency virus

LPS: Lipopolysaccharides

LUVs: Large unilamellar vesicles

MDR: Multidrug resistance

MIC: Minimum inhibitory concentration

NPN: N-phenyl-1-N-naphthylamine

ONPG: O-nitrophenyl-3-d-galactoside

SPPS: Solid-phase peptide synthesis

SUVs: Small unilamellar vesicles

TFA: Trifluoroacetic acid

TFE: Tetrafluoroethylene

TIS: Triisopropylsilane

VAL: Valinomycin

1. Introduction and goals

Antimicrobial resistance (AMR) allows bacteria to resist the effects of antibiotics, posing a risk to public health by making infections harder to treat.¹ Two primary mechanisms contribute to the development of antibiotic resistance in bacteria: intrinsic mechanism and adaptive resistance.² To tackle AMR, several innovative approaches and non-conventional technologies are being developed. (i) new antibiotics with multiple points of action, (ii) antibiotic adjuvants, (iii) monoclonal antibodies and phage therapy, (iv) agents that alter membrane permeability, among others.³⁻⁵

One promising approach for countering resistance is to target the transmembrane electrochemical gradient across bacterial cells, which plays a vital role in various cellular processes, including development of resistance.⁶ The impact of membrane depolarisation by antibiotics is well studied.⁷⁻¹⁰ However, the impact of membrane hyperpolarisation on antibiotic susceptibility is not well understood. Recent studies have shown that some inorganic compounds and antimicrobial peptides (AMPs) can kill bacteria by hyperpolarising the membrane rather than depolarisation.^{11,12}

AMPs are promising candidate which primarily target the bacterial membrane with multiple mechanisms.¹³ AMPs also frequently synergise with clinically relevant antibiotics; Sensitise antibiotic resistant bacteria and the development of resistance against them are limited.¹⁴⁻¹⁹ Again, studies have shown AMPs in combination with antibiotics often show synergism at sub-inhibitory concentrations.^{20,21} Thus, development of novel peptide-based agents which can work at sub-MIC level through membrane hyperpolarisation can be a good strategy to decrease antibiotic resistance in multi-drug resistant pathogens when used in combination with antibiotics.

PGLa, an AMP found in the skin of frogs, may be a promising antimicrobial peptide that could be used as a starting point for the design of a combination therapy agents.¹⁴ It is reported that PGLa works by disrupting the integrity of the bacterial membrane through strong hydrophobic interactions with lipid components, but at low concentrations it can permeabilize the bacterial membrane without forming pores.^{22,23} This leads us to propose that PGLa derivatives with improved properties could potentially disrupt bacterial ion homeostasis and membrane potential at sub-inhibitory concentrations, and work as adjuvants to enhance the sensitivity of antibiotic-resistant bacteria to conventional antibacterial agents. Furthermore, by

introducing β -amino acids into the structure we aimed to reduce hydrophobic stabilisation of the helix-membrane interaction in PGLa molecules, which would promote selective ion transport through the intact membrane.

Another key aspect of this research is to determine if modulation of the bacterial membrane potential is the underlying mechanism behind the effects of AMPs at sub-inhibitory concentrations in general. AMPs have been studied for their membrane lytic mechanisms of action above the minimum inhibitory concentration (MIC).²⁴ But these peptides are often produced in a diluted environment in nature where it may not be possible to reach the MIC level.²⁵ Hence, it is compelling to focus on their action at the sub-MIC level. However, little is known about the underlying mechanism and the bacterial response at sub-inhibitory doses. Therefore, a study that includes a diverse set of AMPs under identical conditions may aid in identifying a possible generalised mechanism at sub-MIC.

Goals

1. To design and synthesise novel peptidomimetic foldamers to enhance antibiotic activity against antibiotic-resistant bacteria and improve resistance to human proteases. We aim to achieve this by using sub-inhibitory concentrations of the new foldamers to decrease bacterial resistance to antibiotics. Our goal was to investigate the mechanism of action of these peptides to determine the validity of our theory regarding membrane potential modulation and ion transport activity.
2. To expand the scope of our membrane potential theory, we set out to investigate 17 diverse cationic peptides meeting various criteria, including their structural diversity, clinical relevance, and different sources. Our objective was to evaluate the effects of these peptides on membrane potential and their abilities to transport both cations and anions under consistent experimental conditions.

2. Literature background

2.1. Antimicrobial resistance (AMR)

AMR, a phenomenon in which microorganisms develop the ability to resist the effects of antimicrobials, is a major global health concern. Multi- and pan-drug resistant bacteria have made it increasingly difficult to treat infections with antibiotics.¹ Bacteria employ two main mechanisms for developing resistance against antibiotics: intrinsic resistance, which arises from natural immunity through native genes, resulting in low membrane permeability and other genetic traits, and adaptive resistance, which occurs due to evolutionary pressure, where bacteria that were once sensitive to antibiotics acquire new genetic material through horizontal gene transfer (HGT) to develop counterattack mechanisms. Different molecular mechanisms include enzymatic degradation or modification, target site alteration, target bypass, decreased influx, active efflux, and target protection.^{2,26}

2.2. Strategies for countering AMR

The current state of AMR and the challenge of discovering new antibiotics necessitate exploring innovative approaches and nonconventional technologies to tackle AMR. Different strategies are being employed to overcome AMR are summarised in Figure 1^{4,27}.

Modulation of bacterial membrane permeability by altering membrane potential can be an approach to effectively overcome antibiotic resistance. The membrane potential, or transmembrane voltage, is the electrical potential difference across a cell membrane. The total bacterial transmembrane potential is the sum of several potential sources explained by models, including the Goldman-Hodgkin-Katz (GHK) model, the Donnan potential, the Nernst potential and the Ohki solution.⁶ Ions such as potassium, sodium, phosphate and chloride are crucial for maintaining bacterial homeostasis. Research has shown that the bacterial membrane potential is crucial for important cellular processes such as membrane transport, motility, cell division, electrical communication, ATP synthesis, and pH homeostasis.²⁸⁻³⁴ Interestingly, disruption of the membrane potential is believed to have a crucial role in the lethality induced by antibiotics.³⁵ One class of agents that can be utilised to target the membrane potential are AMPs.

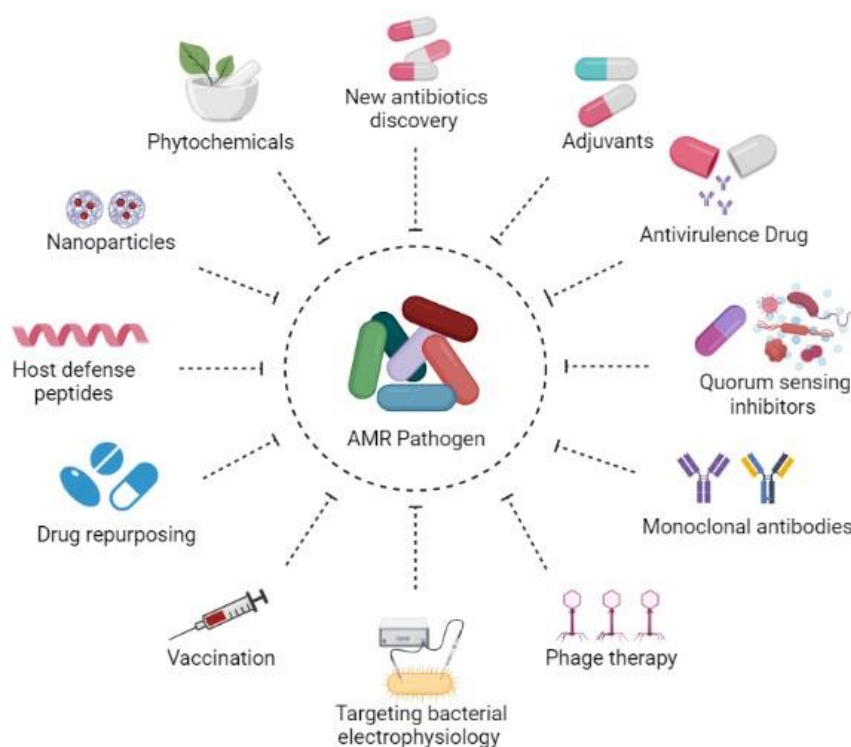


Figure 1: Strategies to counter antibiotic resistance.

2.3. Antimicrobial peptides (AMPs)

Antimicrobial peptides have multifaceted nature and are generated by all forms of complex animals, insects, and plants as a part of their defence mechanism against infections.³⁶ These small cationic amphipathic peptides exhibit moderate effectiveness against a wide range of microorganisms.³⁷ Recent studies have shown that AMPs possess potential not only as antimicrobials but also as antibiofilm, immunomodulatory, and anti-inflammatory agents. Thus, to encompass other activities, these are often referred to as "Host Defence Peptides" (HDPs).^{13,38,39}

2.3.1. Classification

Due to the diverse nature, AMPs can be classified into several categories based on different aspects.⁴⁰ In the aspect of source, AMPs can be derived from natural sources and synthetic sources. Data repository of antimicrobial peptides (DRAMP) contains 6105 entries of natural and synthetic peptides.⁴¹ Secondary structure wise, they can be classified in α -helix (magainin, PGLa, LL37) β - sheet (Protegrins, Tachyplesins), both α -helix and β -sheet (α 1-purothionin), disordered peptides (Indolicidin) (Figure 2). Activity-wise, they can be classified as antibacterial, antiviral, antifungal, antiparasitic, anti-human immunodeficiency virus (HIV) and

antitumour peptides etc. according to another popular data base called APD3.⁴² Depending on the nature of the study, other categories are also mentioned such as anionic / neutral peptides, glycopeptides, cyclic peptides.^{43–46} For this current work, we are highlighting natural and some synthetic classes specifically α/β – peptides.

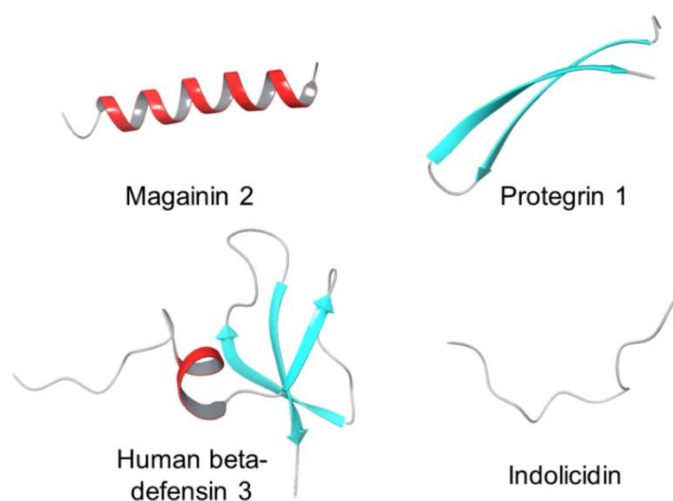


Figure 2: Examples of natural cationic AMPs with different secondary structures.

Most naturally isolated peptides are typically small cationic amphipathic peptides with fewer than 50 amino acids and a net positive charge of +2 to +9 at physiological pH.¹³ It is notable that more than 2,600 natural peptides with highly diverse sequences and structures have been identified.⁴² Natural AMPs can be formed through ribosomal and non-ribosomal peptide synthesis. Most living organisms produce peptides by ribosomal synthesis. However, in microbes, non-ribosomally synthesised peptides can also undergo post-translational / cotranslational modifications. AMPs derived from non-ribosomal synthesis show greater diversity.^{47,48} These modifications may result in improved target recognition and stability, sometimes enhancing their functionality compared to animal-derived ribosomal peptides. These peptides are classified as bacteriocins in recent reviews.⁴⁹ Defensins and cathelicidins are the two primary groups of AMPs in vertebrates. β -defensins found in all vertebrates and produced mainly in epithelial cells, while α -defensins are produced mainly in neutrophils. Cathelicidins are α -helical, amphipathic, and cationic peptides that interact with bacterial membranes, controlling the inflammatory response. Other AMPs, such as histatins and magainin 2, are being studied as antibiotic substitutes. Innate defence mechanisms in plants, fungi, and invertebrates also rely on AMPs, which have distinct secondary structures. Plants produce many

antimicrobial peptides with diverse functions due to gene duplication and evolution, converging with mammalian defensins. Natural AMPs have diverse structures and show promise as antimicrobials, but they are constrained by limitations such as degradation by proteases, potential toxicity to mammalian cells, and high production costs. To overcome these challenges, various chemical modifications have been made to both natural and synthetic AMPs to increase their antimicrobial potency and reduce their vulnerability to proteolysis. Modifications include substitution of amino acid residues, acetylation and amidation of N- and C-terminal, cyclisation, PEGylation, lipidation, creation of hybrid peptides and addition of unnatural amino acids like β -form, d-form etc.⁵⁰

β -peptides are the most researched type of foldamers, synthetic oligomers that tend to form well-defined structures.⁵¹ They are designed to mimic biopolymers in structure and function, making them a promising option for biopharmaceuticals.⁵² Incorporating unnatural β -amino acids into the α -peptide backbone increases its resistance to proteolysis.⁵³ Insertion of a single methylene group α -amino acid leads to β -amino acid. These offer greater diversity due to the additional substitution position and stereogenic centre.⁵⁴ The substitution pattern of the monomers determines whether they are classified as β^2 -, β^3 -, and $\beta^{2,3}$ -amino acids (Figure 3). C_α and C_β atoms have the potential to be in a cycloalkane or heterocyclic ring, resulting in decreased conformational flexibility and increased stability of a specific secondary structure. Both cycloalkane and heterocyclic rings stabilise a given secondary structure. In addition to pure β -peptides, α/β -peptide foldamers can be synthesised by combining β -amino acids with α -peptide chain in a specific pattern ($\alpha\alpha\beta$, $\alpha\alpha\alpha\beta$, $\alpha\alpha\beta\alpha\alpha\beta$), preserving α -helical conformation while protecting against degradation.⁵⁵

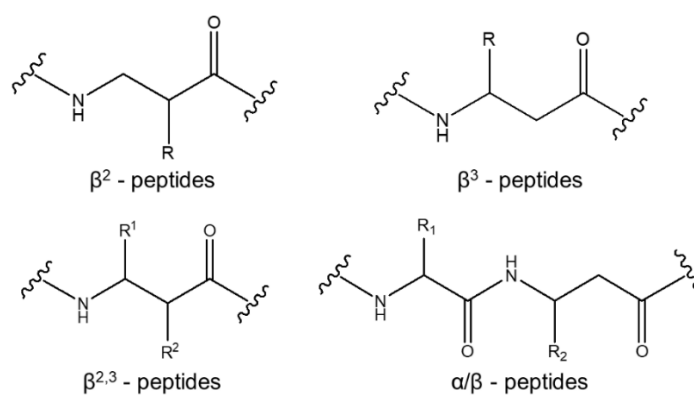


Figure 3: Substitutional pattern of the different β -peptides.

2.3.2. Mechanism of action

To effectively design new AMP therapeutics, it is crucial to understand their mechanisms of action. Research on these peptides has long been centred on their ability to kill bacteria by rupturing or leaking the membranes, which causes cell lysis and death. The precise mechanism by which AMPs damage membranes, including transmembrane pore or nonpore mechanisms, and the effect of peptide concentration on bilayer integrity have been debated by experts in the area. The possibility of ion channel formation by AMPs mechanisms is also discussed. Another broader area of effects of AMPs is the immune modulation ability which has gained a lot of attention lately. It is plausible that AMPs use multiple modes of action simultaneously in various situations.⁵⁶

2.3.2.1. Membrane disruption/ depolarisation

AMPs disrupt membranes through differences in the composition of host and pathogen membranes. Mammalian cells have neutral phospholipids, whereas bacterial membranes have negatively charged phospholipids such as phosphatidylserine and cardiolipin. Gram-positive bacteria have negatively charged teichoic acid and Gram-negative bacteria have negatively charged LPS on their outer membrane. This negative charge on bacterial surfaces causes electrostatic binding with cationic peptides.⁵⁶ While some AMPs are cationic, allowing them to exploit the negative charge of bacterial surfaces through electrostatic attraction, others are anionic and rely on hydrophobicity, positively charged N-terminus to interact with the membrane or by membrane transporter protein.⁵⁷⁻⁵⁹ Most AMPs are also amphipathic, allowing them to interact with the membrane by balancing polar and hydrophobic residues.⁶⁰ The peptide to lipid ratio on the cell surface increases either to charge or membrane component interaction, and when a threshold concentration is attained, peptides usually insert into the hydrophobic membrane.⁶¹ After initial interaction, AMPs can cause membrane disruption through four mechanisms based on studies of model membranes: barrel-stave, toroidal, carpet, or aggregates (Figure 4).⁶² In the barrel-stave model (a variation of the aggregate model), the peptides act as staves and vertically insert themselves into the membrane as a pore, disrupting its structure. The toroidal model forms a pore like the barrel-stave model, but the peptides cause local membrane thinning and curvature, disrupting the membrane. In the carpet model, peptides cover the negatively charged membrane on the basis of electrostatic attraction, and the membrane above

the threshold concentration ruptures in a detergent-like manner forming peptide-lipid micelles. In the aggregate model, peptides form transient and leaky aggregate structures to reach intercellular targets.

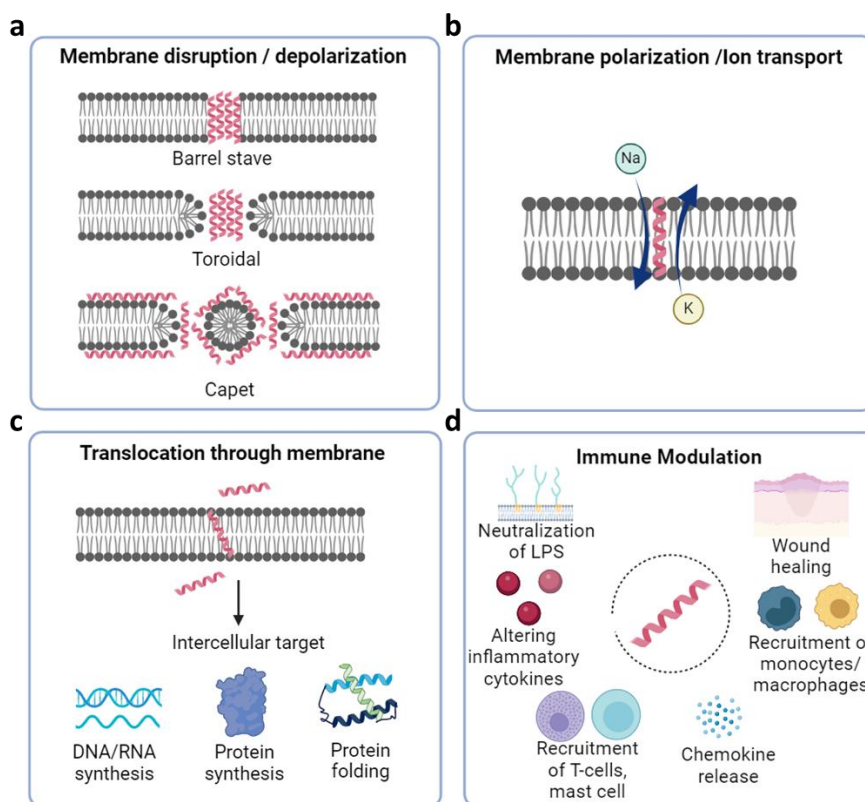


Figure 4: Summary the reported mechanism of AMPs.⁶³

2.3.2.2. Ion channel formation

The ability of peptides to form ion channels has been recognised for a long time, beginning with the discovery of alamethicin. Over the years, several peptides have been found to form cation or anion or both type of channels. In many studies, K⁺ efflux is described as loss of membrane integrity. In contrast, other studies suggested that peptides can transport ions without creating non-selective pores. Gramicidins are short polypeptides produced by *Bacillus brevis* that are well known to form ion channels by dimerising to form an unusual β -helix nanopore that spans the membrane. This allows monovalent cations such as Na⁺ and K⁺ to freely diffuse through, leading to membrane depolarisation, osmotic swelling, and cell lysis.^{64,65} Valinomycin, 36-membered cyclododecapeptide, composed of alternating peptide and ester linkages, creating a hydrophobic surface and a polar cavity that can coordinate with one

K^+ , forming a valinomycin- K^+ complex that incorporates into biological bilayer membranes, transporting K^+ through the membrane and dissipating the membrane potential, ultimately killing cells.⁶⁶ Recent study demonstrated that valinomycin- K^+ complex creates an ion pair with anions with low solvation energies like ClO_4^- , this makes it easy for the ion pair to enter the hydrophobic region of the bilayer transporting the cation across the membrane.⁶⁷ Other peptides have been compared to these two models to explain their mechanism of action. On the other hand, there are reports that mention the formation of oligomers in the lipid membrane that form a complex channel structure.⁶⁸ Considering the complex structure and selectivity of the ions, a study exploring the similarities of these peptide channels to existing bacteria, such as the Ksca channel mechanism, could be useful. Table 1 lists some studies that report peptides with ion channel activity.

Table 1: List of reported ion channel activity by AMPs.

Peptide	Channel type	Membrane type	Method
Magainin	Anion	POPC:DOPE planer lipid bilayer.	Patch-clamp. ⁶⁹
Tachyplesin 1	Potassium	<i>Staphylococcus aureus</i> and <i>Escherichia coli</i> .	Potassium electrode. ⁷⁰
Protegin 1	Potassium	<i>Escherichia coli</i> and methicillin-resistant <i>Staphylococcus aureus</i> .	Potassium electrode. ⁷¹
	Both cation and anion	Planer membrane; POPC/POPG vesicles.	Voltage clamps with Ag/AgCl electrodes; potassium micro electrode. ⁷²
	Anion	<i>Xenopus laevis</i> oocytes.	Double-electrode voltage clamp. ⁷³
DOPS/POPE; DOPS/DOPE and DOPS/POPE Planar Lipid Bilayers.		MD simulation; Voltage-clamp. ⁶⁸	
Gramicidin	Potassium	<i>Staphylococcus aureus</i> and <i>Escherichia coli</i> .	Potassium electrode. ⁷⁴
Defensins	Voltage dependent weekly anionic	Soybean phosphatidylethanolamine, soybean phosphatidylcholine, and bovine phosphatidylserine planer bilayer.	Ag/AgCl electrodes. ⁷⁵
Melittin	Potassium	<i>Staphylococcus aureus</i> and <i>Escherichia coli</i> .	Potassium electrode. ⁷⁴
Histatin 5	Potassium	Yeast cells <i>Candida albicans</i> .	Atomic absorption spectroscopy. ⁷⁶
Synthetic NP108	Potassium	<i>Escherichia coli</i> .	Atomic absorption spectroscopy. ⁷⁷
Plicatamide	Potassium/ Selective cation	<i>Staphylococcus aureus</i> ; Planer lipid bilayer membrane from <i>Escherichia coli</i> lipids.	Potassium electrode; Voltage clamps. ⁷⁸
SMAP-29	Potassium	<i>Escherichia coli</i> and methicillin-resistant <i>Staphylococcus aureus</i> .	Potassium electrode. ⁷¹
HP (2–20)	Potassium	<i>Candida albicans</i> .	Inductively coupled plasma mass spectrometer. ⁷⁹
Aurein 2.2 and 2.3	Cation	<i>Bacillus subtilis</i> ; DPPG/DPPE vesicles.	Inductively coupled plasma atomic emission spectroscopy; Fluorescence measurement with pH-sensitive dye pyranine. ⁸⁰
Tritrpticin	Potassium/ Selective cation	Planar lipid bilayers formed from azolectin or from DPhPC.	Voltage-clamp. ⁸¹
Cecropin A	Potassium	<i>Staphylococcus aureus</i> and <i>Escherichia coli</i> .	Potassium electrode. ⁷⁴
ORB 1	Anion selective	DOPG/DOPE vesicles.	Fluorescence-based transmembrane transport assays using lucigenin and HPTS. ⁸²
Carnocyclin A	Anion selective	POPE: POPS: POPC planer membrane; CcIA liposomes.	Ag/AgCl electrode. ⁸³
Cryptdin 3	Anion selective	Cytoplasmic membranes of human embryonic kidney cells.	Inside-out patch-clamp. ⁸⁴
Gaegurin 4	Slightly potassium selective	PE:PC or PE:PS planar lipid bilayer.	Voltage-clamps. ⁸⁵

2.3.2.3. Intracellular targets

In addition to gross damage to the bacterial membrane, AMPs have also been reported to target DNA; RNA; protein biosynthesis and metabolism; protein folding; cell wall biosynthesis; cell division; proteases, etc.⁸⁶ Buforin II, a 21-amino acid fragment, can permeate the membrane of *E. coli* without causing cell lysis. It interferes with DNA and RNA metabolism by binding to nucleic acids.⁸⁷ Indolicidin targets DNA, crosslinks with single or double-stranded DNA, and inactivates DNA topoisomerase I, inhibiting DNA replication and transcription.⁸⁸ Tachyplesin with antiparallel β -sheet structure binds to the minor groove of DNA duplex.⁸⁹ AMPs such as Bac7, Pleurocidin, PR-39 and CP10A inhibit bacterial cell growth by interfering with ribosomes, DNA and RNA synthesis.⁹⁰⁻⁹² A group of proline-rich AMPs from insects, such as pyrrhocoricin, apidaecin and drosocin, can inhibit bacterial growth by interrupting the protein folding pathway.^{93,94} The human α -defensin 5 (HD5) can enter the cytosol of bacteria and induce multiple cellular damage, including elongation and clumping of cells.⁹⁵ Mersacidin interfere with cell wall biosynthesis via targeting the peptidoglycan biosynthesis pathway.^{96,97}

2.3.2.4. Immune modulation

AMPs are also known to play an important role in interacting with the host immune system to modulate the inflammatory response. Early studies on AMPs focused on its nonmicrobicidal properties and its effects on immune cells, particularly its ability to recruit leukocytes.⁹⁸ But new studies reveal a diverse range of functions which appear to be influenced by various factors such as the environment, cell and tissue type, and AMP concentration. The molecular mechanisms underlying the ability of AMPs to modulate the immune system are complex and involve various cellular receptors, intracellular interacting proteins and signalling pathways, and transcription factors.¹³ AMPs are known to recruit immune cells such as neutrophils, macrophages, mast cells, and T cells and also indirectly promote leukocyte recruitment by inducing the release of chemokines.⁹⁹⁻¹⁰¹ Some natural AMPs have been shown to neutralise inflammation caused by LPS in in vitro and in vivo models.¹⁰² Polymyxins are cationic lipopeptides that can modulate inflammatory cytokines by directly binding to LPS.¹⁰³ Further research is needed to fully understand the mechanisms behind the selective ability of AMP to modulate the immune system and protect against infections, resolve inflammation and maintain immune homeostasis.

2.3.3. Systems for studying membrane activity

To understand the membrane activity of the peptides, (i) synthetic unilamellar bilayers (i.e., one bilayer) such as small unilamellar vesicles (SUVs), large unilamellar vesicles (LUVs), giant unilamellar vesicles (GUVs) and planar supported bilayers; (ii) molecular dynamics simulations studying peptide-membrane interactions; (iii) biological membrane systems are utilised.²⁴

LUVs are the most commonly used artificial membrane structures that can be manipulated to more closely resemble biological membranes by adding specific lipids. LUVs are used to study membrane permeabilising peptides in a controlled and reproducible way, making them an excellent model for studying physicochemical properties that are difficult to observe in biological systems or with molecular dynamics. The most widely used methods for measuring the permeabilisation of LUVs involve leakage assays, which can be tested using light scattering, electron spin resonance, or fluorescence spectroscopy, as well as nuclear magnetic resonance and other methods. Carboxyfluorescein dyes are used to quantify their direct leakage from LUVs, while potential-sensitive dyes such as 3,3'-diethylthiadicarbocyanine iodide [DiSC2(5)] are used to gauge the movement of ions such as K^+ .^{104,105} In the study of how peptides interact with planar bilayers, various electrodes are used to monitor voltage changes, while atomic force microscopy (AFM) is used to visualise membrane rearrangement and pores.^{106,107} Electrochemical impedance spectroscopy (EIS) can provide measurements of bilayer electrical properties, resistance, and capacitance, as well as monitor the permeability of a membrane to small ions such as Na^+ , K^+ and Cl^- .¹⁰⁸

To understand the permeabilisation properties of biological membranes, a direct measurement of bacterial membrane permeabilisation is necessary, as biophysical membranes cannot fully recreate these properties. The leakage of polar compounds or proteins out of the cell or the entry of polar compounds into the cell can be used to measure the permeabilisation of the bacterial membrane. The N-phenyl-1-N-naphthylamine (NPN) uptake assay and the O-nitrophenyl-3-d-galactoside (ONPG) influx method can quantify the permeabilisation of the outer and inner membrane of Gram-negative bacteria, respectively. Disruption of ion gradients across bacterial membranes can be measured using sensitive dyes with.¹⁰⁹ Various peptides have been studied using broth dilution, radial diffusion, haemolysis, NPN uptake, ONPG influx assays, and electron microscopy.^{22,110-112}

2.3.4. Advantages of AMPs

2.3.4.1. The therapeutic potential of AMPs

Due to their broad-spectrum bactericidal, wound healing, antibiofilm, and angiogenesis capabilities, AMPs have been recognised as possible therapeutic agents for a variety of infections.¹¹³ Many peptide-based therapeutics are currently in clinical trials aimed primarily at treating infections such as respiratory tract, oral, and catheter-related infections, and for wound healing.⁴¹ AMPs have been successfully used to heal infected wounds in *in vitro* and animal models. For example, in a mouse model, the new DRGN-1 peptide, which was created from the plasma of a Komodo dragon, demonstrated considerable inhibition of mixed-species biofilms and enhanced wound healing.¹¹⁴ It has been demonstrated that the horseshoe crab-derived substance tachyplesin 3 has been shown to improve phagocytic activity *in vitro* and reduces drug resistant bacterial counts and levels of pro-inflammatory cytokines in mice.¹¹⁵ Some AMPs are also in the clinical trial phase. For the treatment of ventilator-associated bacterial pneumonia, murepavadin, a peptidomimetic based on the cationic AMP protegrin 1, has successfully completed phase 2 clinical trials. A high amount of bactericidal activity against oral infections and biofilm elimination abilities have been demonstrated by the synthetic cationic AMP Nal-P-113.¹¹⁶

2.3.4.2. Synergism with antibiotics

Combination chemotherapy is often favoured in the treatment of complex infections over the use of a single antibiotic due to its reduced likelihood of drug resistance. This is because multiple antibiotics simultaneously target the infection in different pathways, making it more effective and slower to develop resistance. Studies have summarised the beneficial interactions between AMPs and conventional antibiotics, with natural and synthetic peptides.^{117,118} Rifampicin and imipenem are the most commonly used antibiotics in combination with AMPs. Nisin, LL-37, HBD and their variants are evaluated and optimised mainly from the AMP side. Synergy between AMPs and antibiotics extends the duration of use of conventional antibiotics, enhances their selectivity, and reduces dosage, limiting side effects and toxicity, and curbing the spread of infections.¹¹⁹ Coordination of bacterial strains, AMPs, and antibiotics is necessary for synergy to occur, with AMPs with strong membrane activity (such PG-1 and HBD-3) having

high synergy with antibiotics that have intracellular targets (such as amikacin and azithromycin).²⁰

The mechanism behind the synergistic effects between AMPs and antibiotics mainly involves changing the permeability of the bacterial cell membrane, allowing antibiotics to access and interact with their intracellular targets. AMPs can interfere with the composition and function of the bacterial cell membrane, increasing its permeability to antibiotics and making it more sensitive to their effects.²⁰ Some AMPs target lipopolysaccharides (LPS) in the outer membrane of Gram-negative bacteria, destabilising its structure and leading to the death of the bacteria.^{119–121} AMPs can also inhibit the metabolic pathways of bacteria, blocking the activity of DNA polymerase, ATP-dependent enzymes, and protein, RNA, and DNA synthesis processes.^{122,123} Some AMPs inhibit enzymes belonging to both classes of aminoglycoside phosphotransferase and aminoglycoside acetyltransferase, which phosphorylate aminoglycoside antibiotics.¹²⁴ AMPs can also hinder bacterial cell wall synthesis and block bacterial efflux pumps, promoting the accumulation of antibiotics in the cell.^{125–127}

2.3.4.3. Synergism with other AMPs

Synergy between AMPs is a naturally occurring phenomenon that can result in antibacterial, antitumor, and immunomodulatory effects.^{128,129} The combined effects of the numerous AMPs found in both animals and plants increase the bactericidal efficacy and broaden the antimicrobial spectrum.¹³⁰ Synergy can be mediated by different peptides in the same geographical area.¹³¹ One of the most studied pair of peptides is PGLa and Magainin 2, belonging to the same magainin family.^{132,133} These peptides demonstrated potent synergistic antimicrobial effects on modified reverse-osmosis membranes, inhibiting *P. aeruginosa* growth and delaying biofilm formation. This can be useful in preventing the formation of biofilms on surfaces and can improve the performance of medical devices, reducing the risk of hospital-acquired infections.

The synergistic effects of AMPs have also been confirmed among peptides derived from different species.¹³⁴ There is a synergy between bacteriocins and AMPs in mammals. The growth inhibitory potency of eukaryotic AMPs pleurocidin against *E. coli* was increased approximately four times when combined with prokaryotic AMPs, pediocin PA-1, sakacin P,

and curvacin A at the nanomolar level, indicating that these AMPs function highly synergistically with pleurocidin.¹³⁵

2.3.5. Sub-MIC activity of AMPs

The impact of subinhibitory concentrations of AMPs on bacterial cell physiology is most under-investigated. In many cases, it can be challenging to reach the bactericidal or fungicidal concentrations necessary for an effective response, since AMPs are frequently diluted in the surrounding environment.²⁵ The effects of conventional antibiotics at subinhibitory concentrations have been well studied and have been shown to trigger unexpected responses from bacterial populations. The sub-MIC effects of AMPs are understudied. However, existing studies indicate numerous positive impacts of sub-MIC AMPs such as inhibition of biofilm formation in Gram-negative bacteria such as *S. aureus* by LL37, Indolicidin, Bovicin HC5, Subtilosin and Nisin;¹³⁶⁻¹⁴⁰ disruption of anionic lipid structure in ExPortal, impacting cysteine protease and cytolysin secretion Polymyxin B and HNP-1;^{141,142} reduction of TSS toxin-1 production by Hg-1,2 and cyclic dipeptides cyclo(1-Phe-1-Pro). Again, they also have synergistic effects with antibiotics (discussed in Section 2.5.2).^{143,144} However, negative effects have also been reported in some cases.¹⁴⁵⁻¹⁴⁷

The effects of AMPs on microorganisms are complex and non-linear. The lack of understanding of the triggering mechanisms behind sub-MIC effects makes it challenging to predict the response. The permeabilisation of the bacterial membrane by peptides are a commonly reported effect in studies. At subinhibitory concentrations, AMPs often caused hyperpolarisation of the membrane in contrast to the widely believed depolarisation mechanism. Table 2 summarises the reports of AMPs causing hyperpolarisation. TP4 caused both hyperpolarisation and membrane potential depolarisation in *Pseudomonas aeruginosa*, while AMPs such as GW-Q6 and SNAPPs caused transient hyperpolarisation. The alteration in the mechanism of action from nonlytic / membrane hyperpolarisation to membrane disruption/depolarisation was observed in the Chex-Arg20 monomer due to its dimerisation and tetramerisation. However, other effects and mechanisms are likely to be involved, such as intracellular targets and gene regulation. Understanding these factors is limited. To fully harness the therapeutic potential of antimicrobial peptides, it is crucial to investigate their nonlethal impacts on microorganisms' physiology and behaviour, in addition to exploring their lethal mechanisms.

Table 2: List of reported hyperpolarisation incidents by peptide.

Peptide	Membrane type	Method
Guavanin 2	<i>Escherichia coli</i>	Flow cytometry with membrane potential-sensitive fluorescent probe DiSC3(5). ¹¹
TP4	<i>Pseudomonas aeruginosa</i>	Membrane potential-sensitive fluorescent probe DiSC3(5). ¹²
Chex-Arg20	<i>Escherichia coli</i>	Flow cytometry with membrane potential-sensitive fluorescent probe DiOC2. ¹⁴⁸
GW-Q6	<i>Pseudomonas aeruginosa</i>	Membrane potential-sensitive fluorescent probe DiSC3(5). ¹⁴⁹
Synthetic peptide RP-1	<i>Salmonella typhimurium</i>	Flow cytometry with membrane potential-sensitive dye DiOC5. ¹⁵⁰
Plant defensin Rs-AFP2	<i>Neurospora crassa</i>	Intracellular microelectrodes. ¹⁵¹
HJH-1	Erythrocyte membrane	membrane potential-sensitive dye DiBAC4(3). ¹⁵²
SNAPPs	<i>Escherichia coli</i>	Flow cytometry with membrane potential-sensitive dye DiOC2(3). ¹⁵³

3. Experimental methods

3.1. Synthesis and purification of Peptides

Peptide Glycine-Leucine (PGL), Cecropin P1 (CP1), LL-37 cathelicidin (LL37), R8 (R8), Indolicidin (IND) were purchased from ProteoGenix. The rest of the peptides were synthesised in the lab.

The peptides PGLb1, PGLb2 and PGLb3 were synthesised using the solid phase peptide synthesis (SPPS) method and manual Fmoc chemistry. The synthesis was performed using Tentagel R RAM resin as the solid support and COMU as the coupling reagent. The coupling duration for alpha residues was 90 minutes with a 5-equivalent amino acid excess, and for β -residues was 180 minutes with a 3-equivalent excess. The other peptides were synthesised using an automatic Liberty Blue synthesiser, with Tentagel R RAM or Wang resin as solid support, depending on the type of C-terminal. The deprotection solution used was 10% piperazine in N-Methyl-2-pyrrolidone (NMP), with N,N'-Diisopropylcarbodiimide (DIC) as activator and Ethyl cyanohydroxyimino acetate (Oxyma) as activator base.

Following synthesis, the cleavage reagent containing a mixture of trifluoroacetic acid (TFA)/water/DL-dithiothreitol (DTT)/triisopropylsilane (TIS) (90 : 5 : 2.5 : 2.5) was used to cleave the peptides for 3 hours. The TFA was then removed through vacuum drying and precipitation in ice-cold diethyl ether. The resin was washed with acetic acid and water, filtered and lyophilized to obtain the peptides in powder form. Purification was performed using RP-HPLC on a C18 column (Phenomenex Luna, 250 \times 10 mm) using a gradient from 0% to 60% over 80 minutes, with a flow rate of 4 mL/min. The eluents A and B used were water (containing 0.1% TFA) and acetonitrile (0.1% TFA) respectively. The purity was confirmed by RP-HPLC and electrospray ionisation mass spectrometry (ESI-MS) measurements using a C18 column (3.6 μ m Aries peptide, 250 \times 4.6 mm) and a gradient from 5% to 80% over 15 minutes, with a flow rate of 0.7 mL/min. The eluents A and B used were water (containing 0.1% HCOOH) and acetonitrile (0.1% HCOOH) respectively.

3.2. Oxidation of peptides with β -sheet secondary structure

The reduced purified peptide powder was dissolved in a 20 mM ammonium acetate solution with a concentration of 100 μ g/mL. The pH was adjusted to 7.4 using NaOH. The solution was placed in a glass vial with the lid open for 48 hours to allow oxidation in air. The completion of the oxidation process was confirmed using HPLC-MS. The peptide was then

purified and lyophilised. The desired formation of disulphide bonds was identified using trypsin and chymotrypsin digestion methods.

3.3. Digestion by trypsin and chymotrypsin

The peptide was dissolved in a 100 mM Tris HCl buffer containing 10 mM CaCl₂, with a pH of 7.8. A stock solution of 1 mg/mL enzyme stock was prepared in a 1 mM HCl buffer containing 2 mM CaCl₂. The appropriate amount of enzyme solution was added to the peptide solution, resulting in a trypsin-to-peptide ratio of 1:20 and a chymotrypsin-to-peptide ratio of 1:60. The mixture was placed in a glass vial on a shaker for 24 hours at 25 °C. The samples were taken at various time points and digestion was stopped by adjusting the pH to 2.0 with 10% trifluoroacetic acid.

3.4. Circular Dichroism (CD) Measurements

The CD spectra of all peptides were analysed using a Jasco J-1100 CD spectrometer. Using a 1 mm quartz cuvette, a scanning rate of 100 nm/min, and 5 accumulations, the measurement was carried out spanning the wavelength range of 260 to 190 nm. A 100 µM peptide stock solution was made in 10 mM Na-phosphate buffer with a pH of 7.2. The LUVs were made the same way as stated in the LUV preparation section, except in 10 mM Na-phosphate buffer without NaCl and with a pH of 7.2. The baseline of solvent was removed from the obtained spectra in both cases of presence or absence of 1 mM LUVs.

3.5. Preparation of large unilamellar vesicles (LUVs)

20 mM LUVs were prepared by mixing 7:3 molar ratio of 1,2-dioleoyl-sn-glycero-3-phosphocholine (DOPC) and 1,2-dioleoyl-sn-glycero-3-phospho-(1'-rac-glycerol) (DOPG) from chloroform stocks in a round-bottom flask. The mixture was purged with nitrogen gas for 20 minutes to form a thin lipid film, which was then dried for 5 minutes using hot air to remove any residual solvents. The film was hydrated with 20 mM HEPES buffer (pH 7.2) containing 100 mM NaCl or NaH₂PO₄ for 1 hour, then kept overnight at 4 °C for the formation of multilamellar vesicles. The vesicles underwent 12 freeze-thaw cycles and were extruded through a 200 nm pore size extruder [Albet Lifesciences] for 12 repetitions. Unencapsulated NaCl or NaH₂PO₄ was removed by dialysis with 20 mM HEPES buffer (pH 7.2) containing 100 mM KCl or NaNO₃ or NaH₂PO₄. The final volume was adjusted to the dialysis buffer and the lipid concentration was determined by a colorimetric assay.¹⁵⁴

The mean particle size and polydispersity index (PDI) of the LUVs were analysed using dynamic light scattering (DLS) method with a zetasizer instrument from Malvern Instruments located in Worcestershire, UK. The 20 mM liposome suspension was diluted to 1:14 with 20 mM HEPES buffer, pH 7.2, containing either 100 mM NaNO₃ or KCl at 37°C, and scanned in 1 cm disposable cuvettes. The zetasizer software was used to analyse the data.

3.6. NMR measurements

A Bruker Ascend 500 spectrometer with a 5 mm BBO Prodigy Probe was used to record the NMR spectra for the ion transport study at a temperature of 310 K. To carry out the ²³Na NMR, 0.5 μL of 1M Dy(PPP)₂⁷⁻ was added to 500 μL of 20 mM LUVs with NaCl (inside) and KCl (outside), as the shift reagent. The ²³Na NMR was run at 132.3124 MHz with a spectral width of 9,091 Hz, 64 data points, and a relaxation delay of 0.1 s. A 90-degree pulse of 10 μs was used. For the ³⁵Cl NMR, 2 μL of 1M Co(NO₃)₂ was added to 500 μL of LUVs with NaCl inside and NaNO₃ outside, as the shift reagent. The ³⁵Cl NMR was run at 49.0091 MHz with a spectral width of 10,000 Hz, 3000 data points, and a relaxation delay of 0.1 s. A 90-degree pulse of 20 μs was used. For the ³¹P NMR, 500 μL of 20 mM LUVs with NaH₂PO₄ inside and NaCl outside was used. The ³¹P NMR was run at 202.474 MHz with a spectral width of 404 Hz, 65536 data points, and a relaxation delay of 0.1 s. A 90-degree pulse of 12 μs was used.

3.7. Membrane polarisation in LUV model

Optima Fluostar plate reader was used for conducting the fluorescence measurements. 0.2 mM LUVs containing 100 mM NaCl (inside) and 100 mM NaCl or 100 mM KCl or 100 mM NaH₂PO₄ or 100 mM NaNO₃ (outside) was used. 1 mg/mL ethanol stock of oxonol VI dye was freshly diluted with the same buffer to maintain a concentration of 0.45 μM in final plate. The excitation and emission wavelength were set to 580 nm and 640 nm respectively with a slit width of 10 nm. Aliquots of 290 μL of the mixture of LUVs and oxonol VI dye were added to Nunc 96-well transparent flat-bottom plates, with three replicates. After the fluorescence stabilized, 10 μL of peptide stock solution was added to each well using a multi-channel pipette. 10 μL buffer was used for the outside background. All measurements were conducted at 37 °C. The fluorescence intensity was normalized as $(F - F_0)/F_0$, where F is the average intensity of the peptides and F₀ is the average intensity of the buffer cells.

4. Results and discussion

4.1. Designer peptidomimetic foldamers for adjuvant therapy

Adjuvant therapy has been proposed as a promising strategy to overcome antibiotic resistance. AMPs are one promising class of agents which can be used as adjuvants as these have been shown to enhance the effectiveness of antibiotics against resistant microorganisms and they are reported to target bacteria with multiple mechanisms. But the low metabolic stability due to sensitivity to proteolytic degradation, cytotoxicity limits their utilisation.¹⁵⁵

One strategy for improving the efficacy of AMPs is to modify their structure.¹⁵⁶ Research has shown that structurally modifying AMPs can increase their synergy with conventional antibiotics.^{157,158} Modification such as incorporation of unnatural β -amino acids into the natural α -peptide backbone of AMPs in specific pattern can preserve the helical structure but reduce the stronger hydrophobic interaction at the same time. On the other hand, β -amino acids significantly improve their stability against proteolytic activity.¹⁵⁹ PGLa has been found to exhibit synergy with other antibiotics and has been associated with widespread collateral sensitivity.^{14,132} This makes it an excellent choice for optimisation for adjuvant therapy.

4.1.1. Rational design of PGLa analogues

Three analogues of PGLa were designed based on molecular dynamics (MD) simulations performed by Dr. Balázs Jojart and Lukács Németh. Main finding of the study was that PGLa can be divided into three main regions when it interacts with the membrane: (i) cationic face - fully solvated residues with mostly basic side chains, (ii) Ala face - fully desolvated hydrophobic residues that make close contacts with the interior of the bacterial membrane, and (iii) partially solvated face - partially solvated hydrophobic residues. Our goal was to modify the backbone of PGLa to reduce the density of side chains along the hydrophobic sides of the helix to promote ion transport phenomenon while maintaining the helical structure of PGLa, which is essential for its interaction with the membrane.¹⁶⁰ It is known that replacing α -amino acids with β -amino acids evenly along the heptad repeat pattern of α -helices maintains the helical structure,¹⁶¹ while replacing α -amino acids with β -amino acids at residues in close contact with the target disrupts the interaction.¹⁶² Backbone homologation approach is reported for foldameric AMPs with tunable and enhanced characteristics.^{159,163,164} Thus, we developed

and synthesized backbone homologated sequences, PGLb1 (cationic face), PGLb2 (partially solvated face) and PGLb3 (hydrophobic face) (Figure 5).

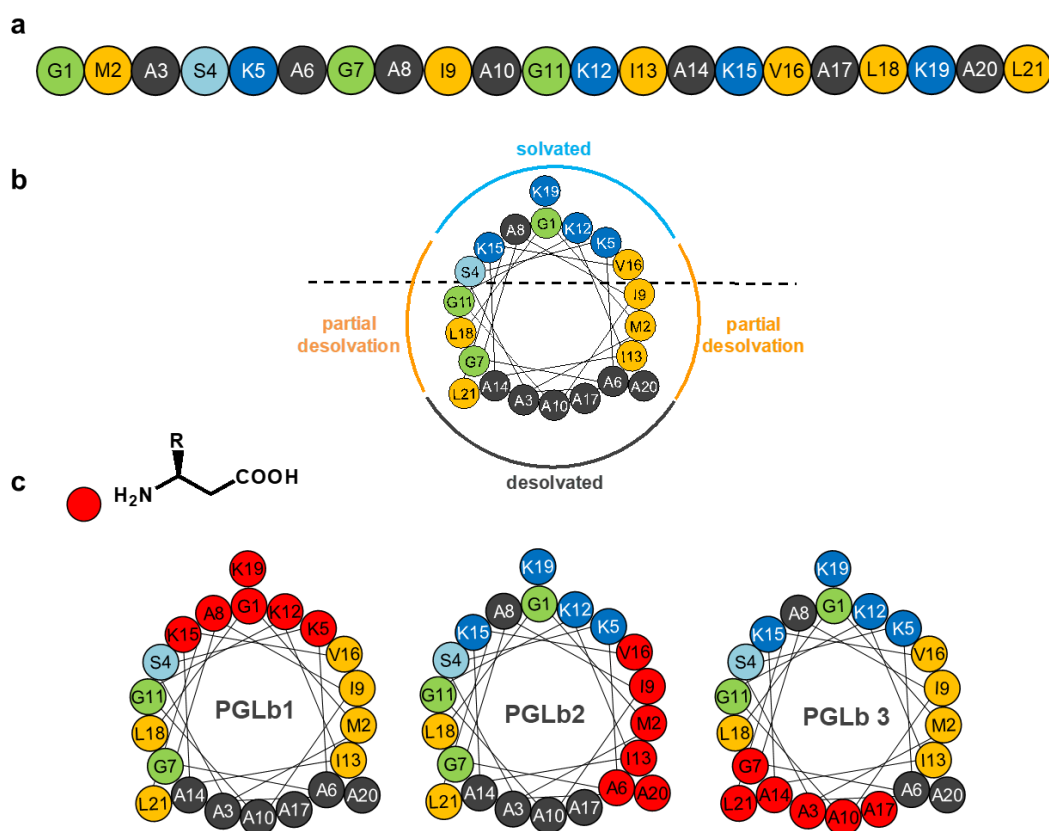


Figure 5: PGLa and the designed foldamers analogues. (a) The sequence of PGLa. (b) different solvation states of PGLa helix. Dash line represents the membrane outer layer (c) Modification positions (homologous $\alpha \rightarrow \beta^3$ amino acid replacements marked by red colour): PGLb1, PGLb2, and PGLb3.

We then performed CD spectroscopy to evaluate whether these molecules still had the ability to form a helix upon interaction with a membrane. CD spectra of each molecule was measured in the presence and absence of DOPC/DOPG LUVs, which are frequently used as models for mimicking biological membranes.¹⁶⁵ In absence of LUVs, all peptide sequences displayed a random coil curve (Figure 6a). When 1 mM LUVs were added, PGLa displayed the typical CD curve for α -helix molecules, whereas PGLa analogues showed a change from a U-shaped CD fingerprint to a cotton-effect with a negative lobe at around 205 nm, indicating the formation of α/β sequences (Figure 6b). These findings indicate that the membrane-induced folding of the PGLa analogues was not significantly affected by the backbone homologation.

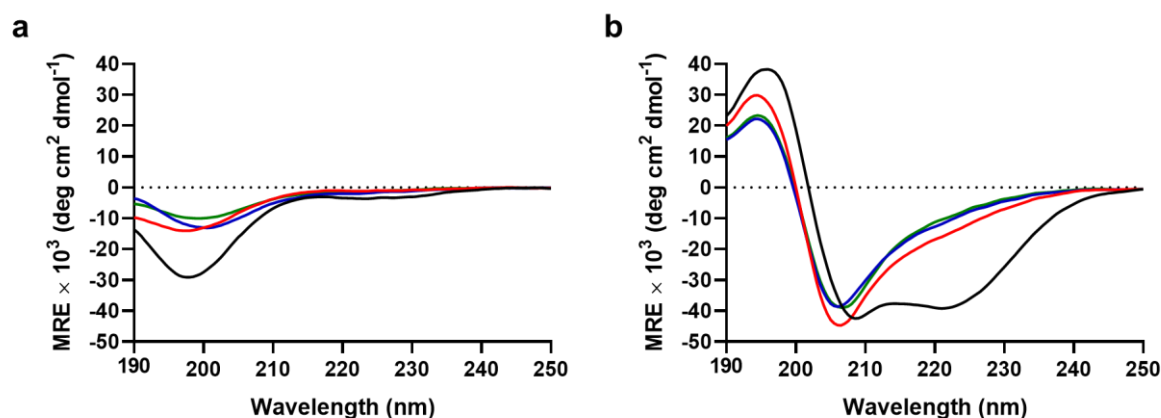


Figure 6: CD spectra of peptides. PGLa (black), PGLb1 (red), PGLb2 (blue), and PGLb3 (green) (a) in absence of LUVs, (b) in presence of 1 mM DOPC/DOPG LUVs.

Biological measurements were conducted by Dr. Csaba Pál and his group. A preliminary measurement of MIC for all sequences against *E. coli* BW25113 was done. The results showed that PGLb1 and PGLb2 (MIC 24 and 19 $\mu\text{g/mL}$ respectively) had retained comparable antimicrobial activity to the parent sequence PGLa (MIC 9 $\mu\text{g/mL}$). However, PGLb3 had almost no antibacterial activity against *E. coli* BW25113 (MIC >200 $\mu\text{g/mL}$), indicating that altering the desolvated ala phase which interacts closely with the membrane is detrimental to the sequence (Figure 7). Therefore, PGLb3 was eliminated from further study.

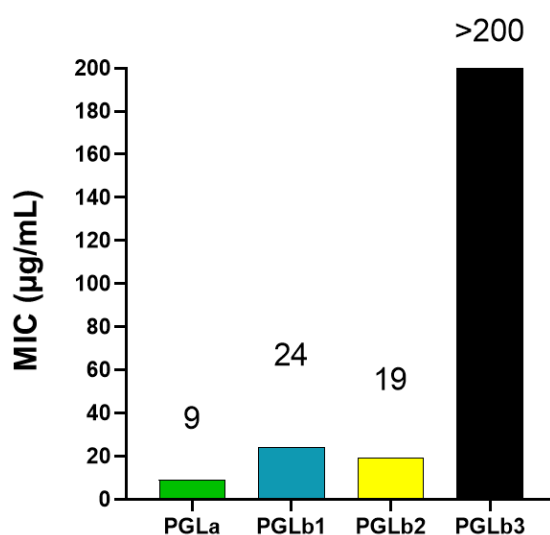


Figure 7: Minimum inhibitory concentrations of PGLa, PGLb1, PGLb2 and PGLb3 against of *E. coli* BW25113.

4.1.2. Foldamers synergize with antibiotics

Following the initial MIC tests, we sought to determine whether the foldamers had additive or synergistic effects when used in combination with nalidixic acid. Nalidixic acid is a DNA synthesis inhibitor. To evaluate these interactions, we examined the impact of various foldamer-antibiotic combinations on the growth of multiple *E. coli* isolates. We used the Loewe additivity model, which the level of interaction between drugs based on the deviation from the expected effect of each drug when used alone.¹⁶⁶ PGLb1 and PGLb2 displayed strong synergism when combined with nalidixic acid, while PGLa had mainly additive effects with nalidixic acid (Figure 8).

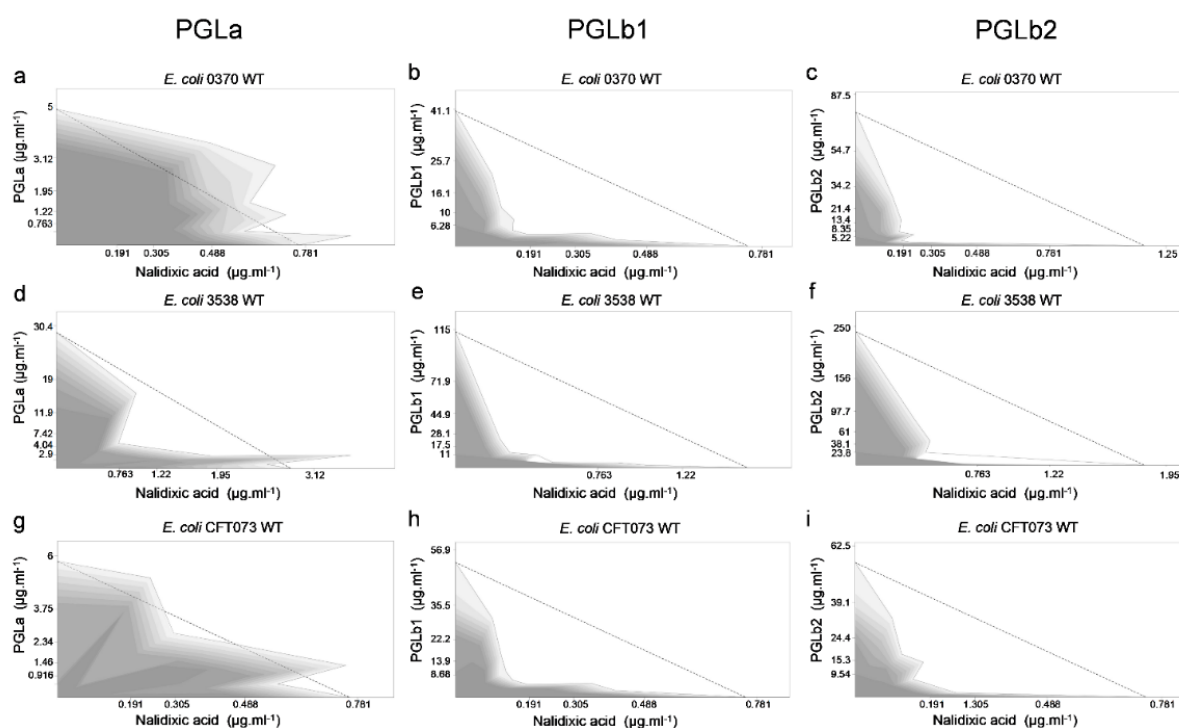


Figure 8: Interactions between Peptides and Nalidixic Acid. (a-c) wild-type *E. coli* 0370, (d-f) *E. coli* 3538 and (g-i) *E. coli* CFT073 strains. Grey shade represents the growth rate of the bacteria with darker shades indicating higher growth rates. The dashed line represents no interaction.

4.1.3. Foldamers restore antibiotic activity in antibiotic-resistant bacteria

Based on our previous findings, we hypothesized that PGLb1 and PGLb2 could effectively combat drug-resistant pathogenic bacteria when used in combination with

antibiotics. To test this hypothesis, we used clinical isolates of *E. coli*, *K. pneumoniae*, and *S. flexneri*, all of which display clinically significant levels of resistance to nalidixic acid. We administered PGLb1 and PGLb2 at sub-inhibitory concentrations ($\frac{1}{2}\times\text{MIC}$ and $\frac{1}{4}\times\text{MIC}$), at a dosage that allowed the growth of the isolates when the peptides were used alone. When used in combination with antibiotics, PGLb1 and PGLb2 significantly decreased resistance to nalidixic acid in all three bacterial species (Figure 9).

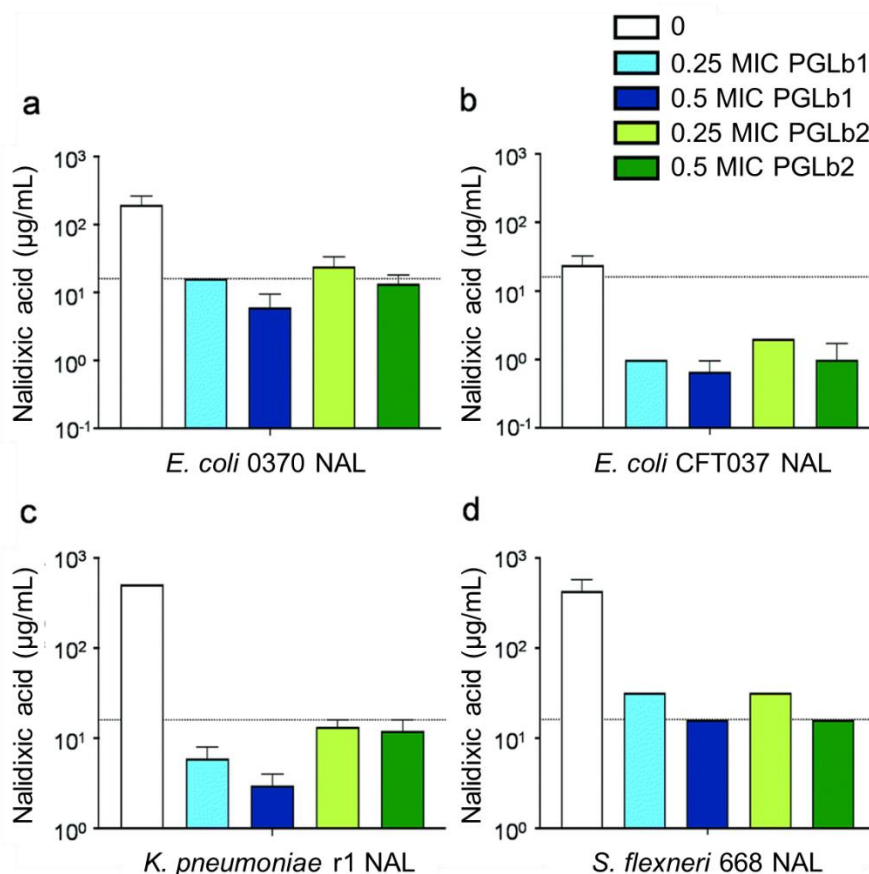


Figure 9: Interaction between foldamers and nalidixic acid. The MIC of nalidixic acid (NAL) was assessed in NAL resistant (a) *E. coli* clinical isolates 0370 and (b) CFT073, (c) *Klebsiella pneumoniae* r1 and (d) *Shigella flexneri* 668 in the presence of $\frac{1}{2}\times\text{MIC}$ and $\frac{1}{4}\times\text{MIC}$ of the peptides. Dashed line represents resistance breakpoint for NAL (i.e., 16mg.l⁻¹) suggested by the CLSI (Clinical Laboratory Standards Institute). Data are based on at least two biological replicates.

4.1.4. Foldamer increased survival rate of *Galleria mellonella* *in vivo*

In vitro data was validated by *in vivo* experiment on larvae of the greater wax moth *G. mellonella*. *G. mellonella* infection models are increasingly popular for testing bacterial

infectivity and compound efficacy because of their high reproducibility and lack of ethical concerns.¹⁶⁷ This established infection model was utilised to evaluate the synergism between nalidixic acid and PGLb1 by assessing their effect on the survival of host larvae. Larvae were infected with a clinical isolates of *E. coli* strain that is resistant to nalidixic acid. When used alone, PGLb1 had no significant impact on the survival of *G. mellonella* ($P = 0.37$). However, when used in combination with nalidixic acid, PGLb1 significantly enhanced the survival of the infected larvae (Figure 10). This indicates that PGLb1 can restore the antibacterial activity of nalidixic acid *in vivo* and increase the survival rate of *G. mellonella*. This study shows that the peptide PGLb1 has potential as an adjuvant to traditional antibiotics in treating drug-resistant bacterial infections.

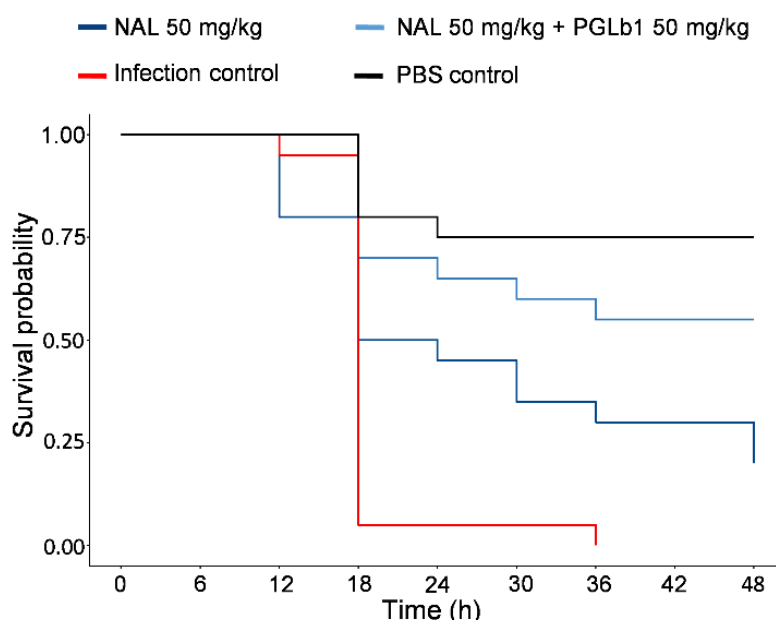


Figure 10: Combination therapy of PGLb1 and nalidixic acid *in vivo*. Experiments were performed in two biological replicates, with 10 animals per treatment group, hence each curve represents 20 animals.

4.1.5. Foldamers trigger hyperpolarisation of *E. coli* membrane

As per literature PGLa exerts its action primarily by targeting the bacterial membrane, thus we theorized that modified analogues PGLb1 and PGLb2 might restore antibiotic activity by interfering with the bacterial membrane potential. Thus, the changes in membrane potential of *E. coli* cells in response to the different sub-inhibitory doses of PGLa, PGLb1, or PGLb2 were measured. Flow cytometric analysis utilising a membrane potential-sensitive dye

DiOC₂(3) was used to measure the membrane potential.¹⁰⁹ All measurements were conducted following 15 or 30 minutes of incubation to prevent any potential bacterial cell death associated with DiOC₂(3). When administered at sub-inhibitory concentrations, PGLb1 and PGLb2 induced substantial and sustained hyperpolarisation of the bacterial membrane, while PGLa had only a relatively mild and transient effect on membrane polarity (Figure 11). Interestingly for the entire experiment, there was no sign of membrane depolarisation caused by PGLb1 or PGLb2 stress, indicating that these molecules do not cause membrane rupture or ion depletion when applied at sub-inhibitory concentrations. In contrast, PGLa depolarized the bacterial membrane after 30 minutes of incubation.

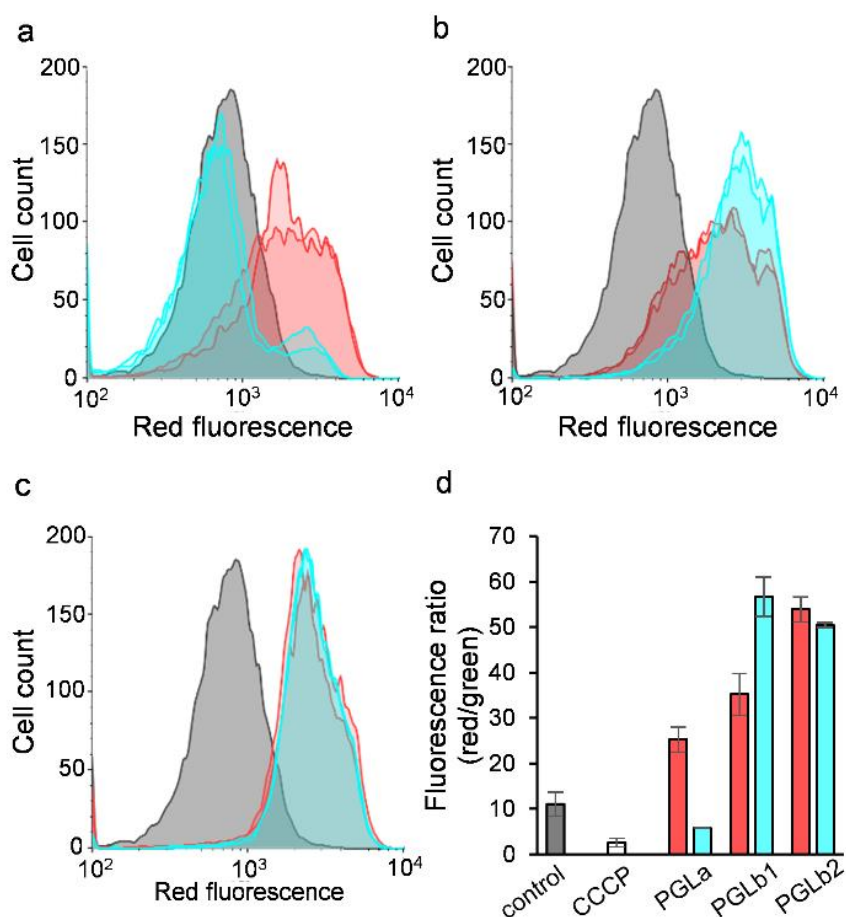


Figure 11: Flow cytometric membrane polarisation assay (BacLight) in *E. coli*. Red channel histograms for (a) PGLa, (b) PGLb1, and (c) PGLb2 are displayed, respectively, after 15 minutes (red) and 30 minutes (blue) of incubation. The control cells are plotted in grey. (d) The ratio of red and green fluorescence represented. CCCP used as depolarising ionophore. Red and blue bars represent measurements after 15 and 30 minutes of incubation, respectively, with a decreased ratio indicating depolarisation and an increased ratio indicating hyperpolarisation.

4.1.6. Foldamers generate diffusion (Goldman-Hodgkin-Katz) potential through selective ion transport

Molecular mechanisms behind the hyperpolarisation of bacterial membranes caused by PGLb1 and PGLb2 was investigated after that. There are two ways in which these peptides can induce a shift in membrane potential in theory: the initial binding of the positively charged regions of these molecules to the negatively charged bacterial membrane, which could shift the static component of the membrane potential, or PGLb1 and PGLb2 acting as selective ion transporters that induce diffusion potential, which is a dynamic process driven by differential ion permeabilities and active ion transport across the membrane.⁶

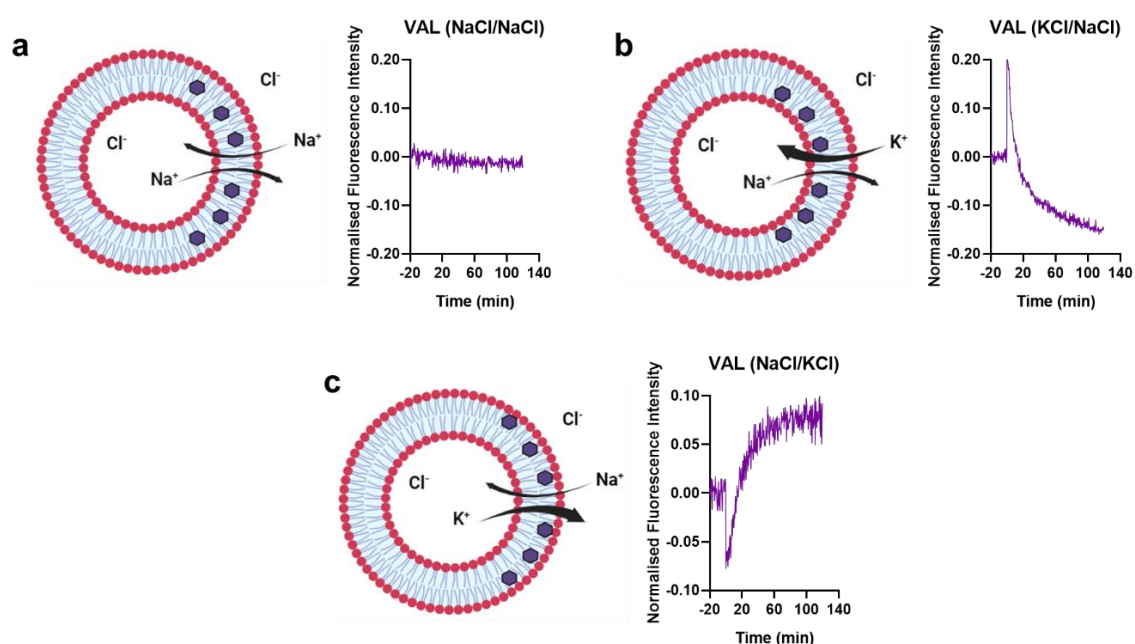


Figure 12: Method validation of membrane polarisation in the LUV model. Membrane polarisation induced by VAL with gradient (a) Na⁺ (outside)/Na⁺ (inside), (b) K⁺ (outside)/Na⁺ (inside), (c) Na⁺ (outside)/ K⁺ (inside). (d) Static potential generated by PGLa, PGLb1, and PGLb2 with Na⁺ (outside)/Na⁺ (inside).

To test these potential molecular mechanisms, a voltage-sensitive dye (oxonol VI) with established LUV model composed of DOPC/DOPG 7 : 3 was used.¹⁶⁸ Valinomycin (VAL), a K⁺-selective ionophore, was used to validate experimental setup (Figure 12). Without an ion gradient (100 mM NaCl outside/100 mM NaCl inside) in LUVs, no fluorescence change was observed, indicating that no static potential was generated by VAL (Figure 12a). When we established a K⁺ (outside)/Na⁺ (inside) ion gradient across the vesicle's bilayer, VAL decreased

the fluorescence level (Figure 12b). This decrease in fluorescence indicates an elevated positive inside membrane potential (diffusion potential) in this LUV system. To further validate the sensitivity of the system, a Na^+ (outside)/ K^+ (inside) ion gradient was created across the LUV membrane, resulting in an increased fluorescence intensity, confirming the experiment's validity (Figure 12c).

When PGLa, PGLb1 and PGLb2 were added without establishing an ion gradient (Na^+/Na^+ environment), we only observed minor increase in the fluorescence level (Figure 13). This suggests that these peptides have only a mild impact on the static component of the membrane potential. However, when a K^+/Na^+ ion gradient was established, these sequences at sub-MIC caused a prompt and significant drop in fluorescence level (Figure 14). This finding indicates the presence of a significant positive inside diffusion potential in the LUV model, facilitated by K^+ -selective ion transport. We also observed a similar decrease in membrane potential when an anion gradient Cl^- (inside)/ NO_3^- (outside) was introduced into the LUV samples, indicating that the sequences can conduct both cations and anions with differential permeabilities. Interestingly, potential generated by the modified sequences PGLb1 and PGLb2 was higher than that of the original PGLa sequence. We observed that the diffusion potential generated by the sequences increased rapidly upon addition and stabilized at a non-zero level or exhibited slow drift after 15 minutes. Our hypothesis suggests that these sequences facilitate minor ion transport, generating voltage without completely dissipating the ion concentration gradient across the membrane which is crucial for maintaining a stable diffusion potential.¹⁶⁹ Achieving equilibrium of intra- and extraventricular ion concentrations would necessitate an effective electroneutral ion exchange across the membrane.

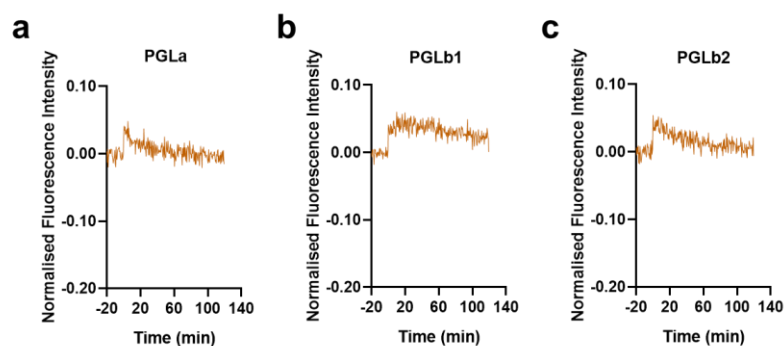


Figure 13: Static potential generated by (a) PGLa, (b) PGLb1, and (c) PGLb2 in LUV model with Na^+ (outside)/ Na^+ (inside).

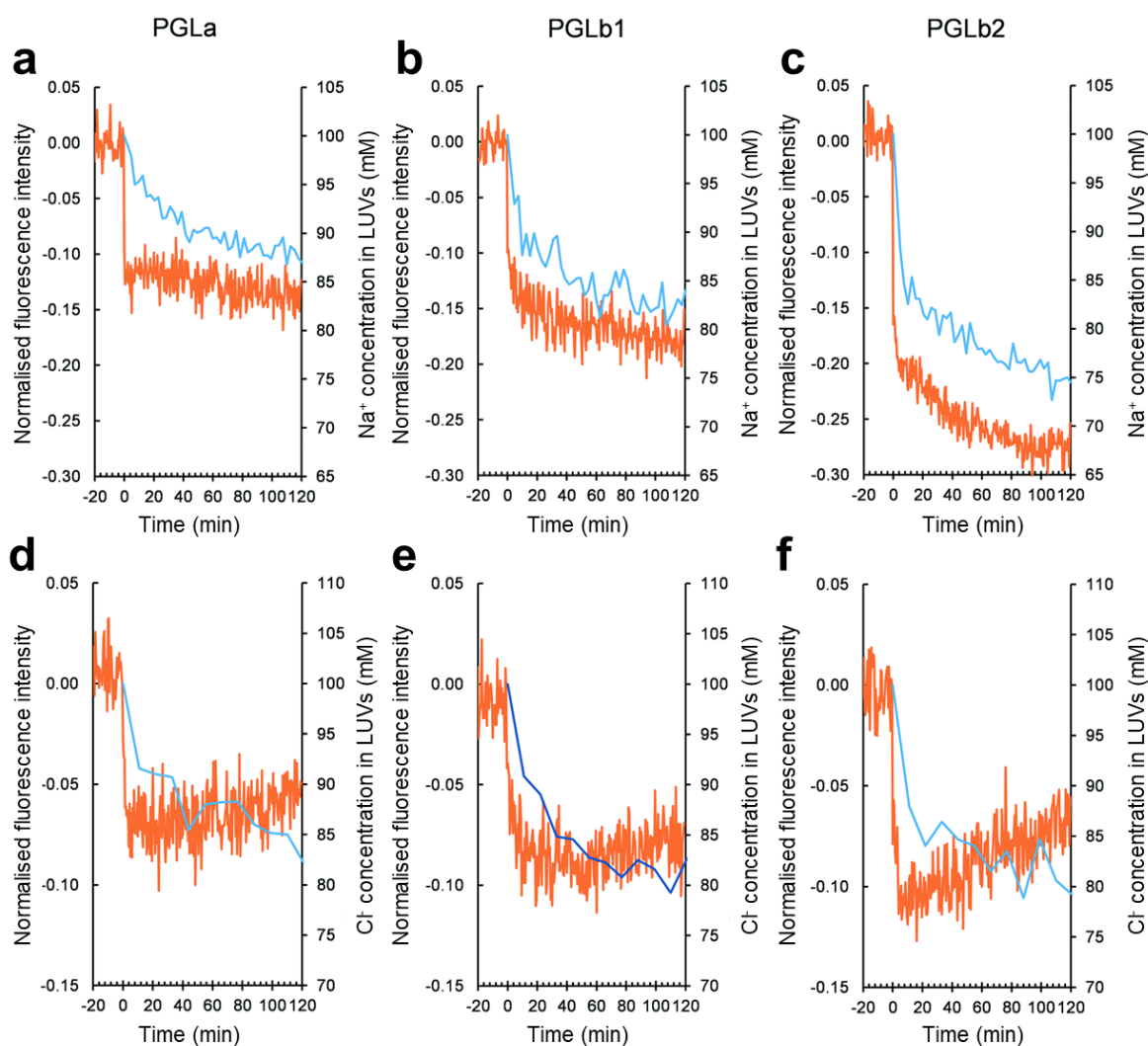


Figure 14: Membrane polarisation and ion transport assessments. Membrane potential (red curve) and inside Na^+ concentration (blue curve) changes are shown in the Na^+/K^+ exchange (100 mM NaCl inside and 100 mM KCl outside) upon adding (a) PGLa, (b) PGLb1 and (c) PGLb2. Membrane potential (red curve) and inside Cl^- concentration (blue curve) changes are shown in the $\text{Cl}^-/\text{NO}_3^-$ exchange (100 mM NaCl inside and 100 mM NaNO_3 outside) upon adding (d) PGLa, (e) PGLb1 and (f) PGLb2.

To assess the level of ion exchange across the bilayer, we directly measured the time-dependent ion concentrations in LUVs using NMR spectroscopy. We used ^{23}Na and ^{35}Cl NMR to detect time-dependent Na^+/K^+ and $\text{Cl}^-/\text{NO}_3^-$ exchanges respectively in identical LUV systems used for fluorescence measurements. When PGLa, PGLb1 and PGLb2 were added, we observed Na^+/K^+ and $\text{Cl}^-/\text{NO}_3^-$ exchanges across the LUV's bilayer surface (Figure 14). There was no transport of shift reagents (Dy^{3+} or Co^{2+}). These findings indicate that PGLa, PGLb1, and PGLb2 induce the flux of single charged ions without rupturing the membrane in the LUV

model when applied at sub-inhibitory concentrations. Similar to membrane potential experiment, ion exchange generated by the modified sequences PGLb1 and PGLb2 was slightly higher than that of the original PGLa sequence. Taken together, these findings support the idea that PGLb1 and PGLb2 hyperpolarize the membrane through selective ion transport, which shape the dynamic diffusion potential.

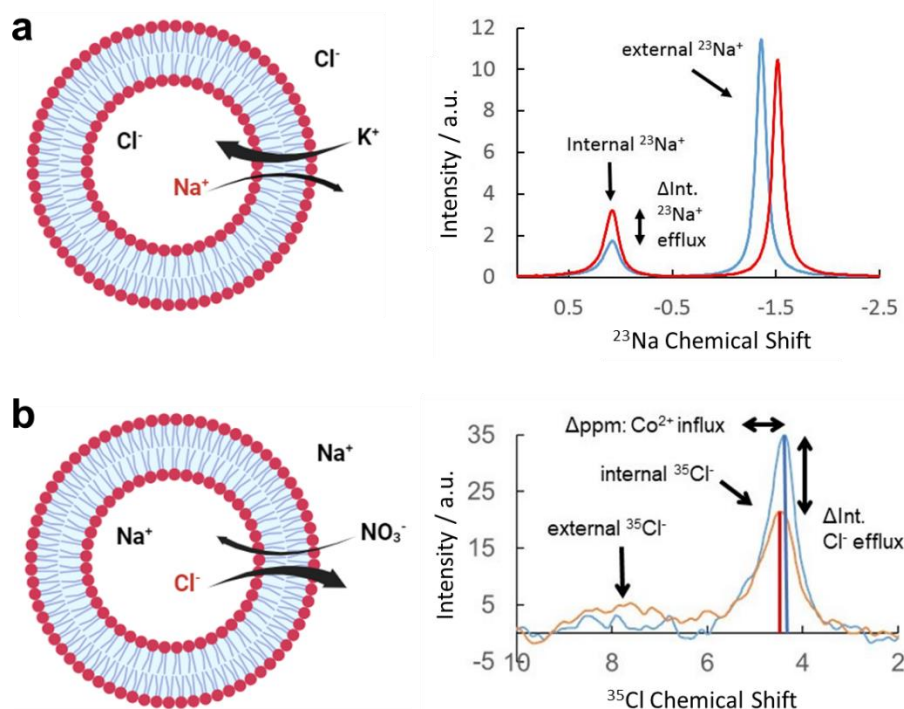


Figure 15: Schematic representation of time-dependent ion transport in the LUV model. (a) Na⁺ transport measurement by ²³Na NMR. In theory, time-dependent Na⁺ efflux can be monitored by observing a decrease in the internal signal in the presence of the shift reagent Dy³⁺. (b) Cl⁻ transport measurement by ³⁵Cl NMR. In theory, time-dependent Cl⁻ efflux without pore formation can be monitored by observing a decrease in the internal signal in the presence of the shift reagent Co²⁺. In contrast, pore formation can be identified by the broadening and shifting of the signal because of the Co²⁺ influx.

4.1.7. Stability and toxicity analyses

The stability of the peptide in the presence of human protease enzymes and potential toxicity are the two key issues with adopting peptide-based drugs as antibiotics. PGLa is readily degraded by human trypsin and proteinase K due to the abundance of lysine molecules in its structure. However, introducing a non-natural β-amino acid into PGLa structure, as in PGLb1 and PGLb2, could improve its resistance to human proteases. We discovered that PGLa

degraded rapidly in the presence of both enzymes, whereas PGLb1 and PGLb2 half-lives significantly increased in the identical conditions (Figure 16a, b). Additionally, we also performed a haemolysis assay on human red blood cells and found that neither PGLb1 nor PGLb2 had an apparent haemolytic impact (<5% haemolysis) (Figure 16c). These results are encouraging, further research is required to thoroughly examine the stability and possible toxicity of these peptidomimetics in the future.

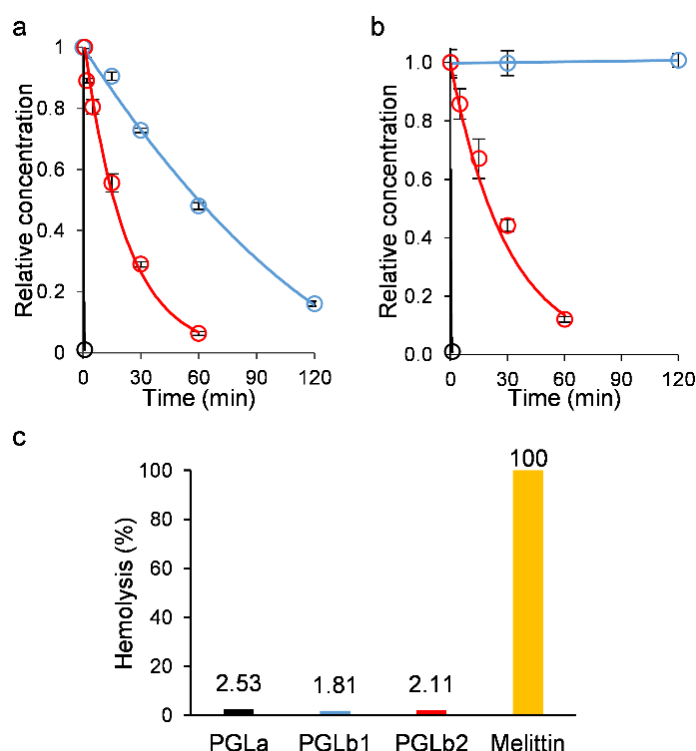


Figure 16: Stability and toxicity assays of peptides. (a) Stability of PGLa (black), PGLb1 (blue) and PGLb2 (red) against trypsin. (b) Stability of PGLa (black), PGLb1 (blue) and PGLb2 (red) against proteinase K. (c) Haemolytic activity of PGLa (black), PGLb1 (blue) and PGLb2 (red) at 500 µg/mL concentration compared to melittin at 50 µg/mL concentration.

4.2. Assessment of a larger landscape of AMPs for membrane polarisation

Although AMPs have been shown to exhibit multiple beneficial biological effects at sub-MIC (discussed in section 2.3.5), there is a lack of knowledge about the triggering mechanisms of these effects. Membrane permeability has been studied extensively for AMPs, but the focus has mainly been on checking for the leakage of cations (mainly, K⁺).⁷¹ There has been a significant lack of research on their ability to transport anions, particularly biologically important anions like chloride and phosphate.

There are sporadic instances of bacterial membrane hyperpolarisation by AMPs (section 2.3.5) and also reports of cationic AMPs causing bacterial membrane-specific ion transport phenomena without causing membrane rupture are mentioned (section 2.3.5). We have shown a link between adjuvant activity of the PGLa based designer peptides at sub-MIC level and their ability to cause hyperpolarisation by ion transport. To further develop this emerging antibacterial adjuvant strategy, a detailed mechanistic understanding of direct chemical-biophysical hyperpolarisation is required. Identifying the structural components of the hyperpolarisation effect at molecular level is essential. Accordingly, we aimed to systematically expand the range of hyperpolarising compounds to ensure sufficient chemical diversity for structure-activity relationship studies. Therefore, we chose to investigate 17 diverse cationic peptides (Table 3) to investigate how they affect the membrane potential and type of ion transport they induce. To achieve diversification, we primarily selected sequences based on their secondary structures, including α -helix, polyproline helix, disulfide-stabilized β -sheet, and disordered sequences. Although we managed to select sequences from different sources like human, animal, plant and synthetic. MIC measurements for all the AMPs were done against *E. coli* BW25113.

Table 3: Information of the AMPs investigated in the study.

Peptides	Abbreviation	Sequence	Source	MIC (μM)*
Apidaecin 1B	AP	GNNRPVYIPQPRPPHRL-OH	Honeybee	9.4
Protegrin-1	PROT1	RGGRLCYRRRFCVCVGR-NH ₂	Pig leukocytes	1.8
Tachyplesin II - Lys	TP2K	KWCFKVCYKGYCKKCK-NH ₂	Arg to Lys modified TP2	1.8
Tachyplesin II	TP2	RWCFRVCYRGICYRKCR-NH ₂	Japanese horseshoe crab	1.7
LL37	LL37	LLGDFFRKSKEKIGKEFKRIVQRIKDFLRNL VPRTE-OH	Human neutrophil	4.2
Indolicidin-OH	IND	ILPWKWPWWPWR-OH	C-terminal modified INDa	10.4
Indolicidin	INDa	ILPWKWPWWPWR-NH ₂	Bovine	4.6
R8	R8	FLGKVFKLASKVFKAVFGKV-OH	Synthetic	6
PGLa - Arg	PGRLa	GMSRAGAIAGRIARVALRAL-NH ₂	Lys to Arg modified PGLa	1.9
PGLa	PGLa	GMASKAGAIAGKIAKVALKAL-NH ₂	African clawed frog	4.6
PGLa-OH	PGL	GMASKAGAIAGKIAKVALKAL-OH	C-terminal modified PGLa	38.1
Guavanin 2	GUA2	RQYMRQIEQALRYGYRISRR-NH ₂	Guava	5.9
Cecropin P1	CP1	SWLSKTAKKLENSAKKRISGIAIAIQGGPR -OH	Pig intestine	0.8
Buforin II	BUF2	TRSSRAGLQFPVGRVHLLRK-OH	Asian toad	102.7
Bactenecin 5	BAC5	RFRPPIRRPPIRPPFYPPFRPPIRPPIFPPIRP PFRPPLGPPF-OH	Bovine	2.6
Magainin II-OH	MAG2	GIGKFLHSAKKFGKAFVGEIMNS-OH	C-terminal modified MAG2a	38
Magainin II	MAG2a	GIGKFLHSAKKFGKAFVGEIMNS-NH ₂	African clawed frog	3.6

*MIC for all sequences tested against *E. coli* BW25113.

The folding dynamics of antimicrobial peptides (AMPs) are often influenced by their environment, particularly by the negatively charged membrane, leading to structural alterations. Therefore, our focus was specifically on examining cationic AMPs with membrane-induced secondary structures. The inducibilities reported in the literature were confirmed by our CD measurements. CD spectra of all AMPs were measured in the presence and absence of DOPC/DOPG LUVs at 0.5 MIC, to evaluate their ability to form secondary structure when come in contact with membrane. Upon adding 1 mM LUVs AP, PROT1, TP2K, TP2, LL37, IND, INDa showed no secondary structural change (Figure 17A). R8, PGRLa, PGLa, PGL,

GUA2, CP1, BAC5, MAG2, MAG2a folded into α -helix structure in presence of LUVs (Figure 17B). BUF2 showed helical structure in Tetrafluoroethylene (TFE) but in presence of LUVs could only show coil structure showing sensitivity process to different condition.

AMPs	Membrane inducibility of the secondary structure	CD curves	Bioactive secondary structure
AP	non-inducible polyproline helix/aggregation ¹⁷⁰		
PROT1	non-inducible β -sheet/aggregation ¹⁷¹		
TP2K	non-inducible β -sheet		
TP2	non-inducible β -sheet ¹⁷²		
LL37	non-inducible stable helix/aggregation ¹⁷³		
IND	non-inducible extended/beta turn		
INDa	non-inducible extended/beta turn ¹⁷⁴		

Figure 17A: Selected AMPs with non-membrane inducible secondary structures. CD spectra were recorded under identical conditions to ensure the reproducibility of the structural features. Coordinates of the secondary structures in the membrane were obtained by molecular modeling using the experimental restraints reported in the relevant citations.

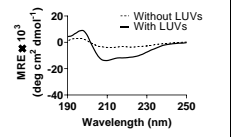
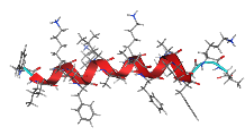
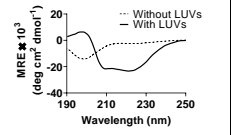
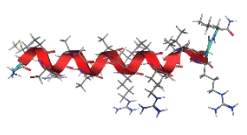
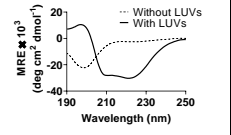
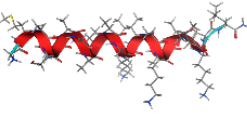
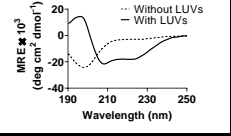
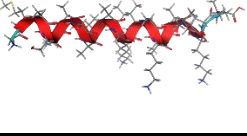
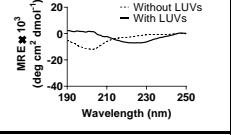
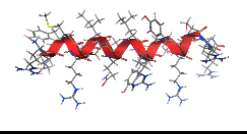
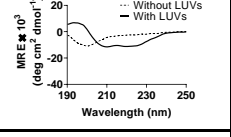
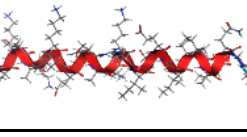
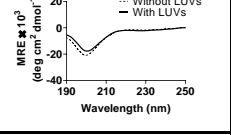
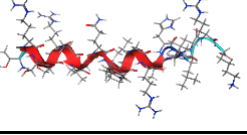
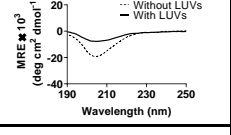
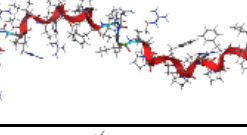
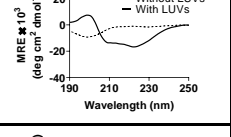
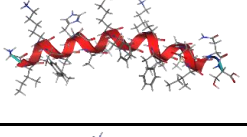
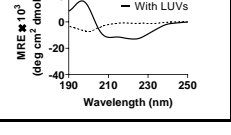
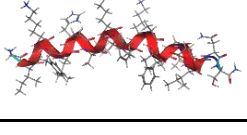
AMPs	Membrane inducibility of the secondary structure	CD curves	Bioactive secondary structure
R8	partially inducible partially disordered → helix ¹⁷⁵		
PGRLa	inducible disordered → helix		
PGLa	inducible disordered → helix ¹⁷⁶		
PGL	inducible disordered → helix		
GUA2	inducible disordered → helix ¹¹		
CP1	inducible disordered → helix ¹⁷⁷		
BUF2	inducible disordered → helix ⁸⁷		
BAC5	inducible extended → polyproline II helix ¹⁷⁸		
MAG2	inducible disordered → helix		
MAG2a	inducible disordered → helix ¹⁷⁷		

Figure 17B: Selected AMPs with membrane inducible secondary structures. CD spectra were recorded under identical conditions to ensure the reproducibility of the structural features. Coordinates of the secondary structures in the membrane were obtained by molecular modeling using the experimental restraints reported in the relevant citations.

4.2.1. Membrane induced AMP structures hyperpolarise *E. coli* membrane at sub-MIC

To test whether AMPs in general induce hyperpolarisation of the bacterial membrane, we measured the changes in the membrane potential of *E. coli* cells in response to AMPs at 0.5 MIC by flow cytometric analysis using the membrane potential sensitive dye DiOC₂(3). To avoid any potential cell death associated with DiOC₂(3), all measurements were run after 15 minutes of incubation. When applied at sub-inhibitory concentrations, MAG2a, MAG2, BAC5, BUF2, CP1, and GUA2 switched the whole bacterium population into a hyperpolarized state. For PGLa, PGL, R8, INDa, and LL37, a bimodal distribution of the membrane polarisation was observed with a significant number of hyperpolarised cells. The rest of the population remained unperturbed or slightly depolarised. AP did not show any significant polarisation of the bacterial membrane (Figure 18).

Many of the AMPs investigated in this study have the capability to induce hyperpolarisation in a sequence-dependent manner. We quantified the median hyperpolarisation values across biological replicates (Figure 18d) and correlated this with the secondary structural characteristics of the sequences (Figure 18e). AMPs with membrane-induced helical structures tend to induce hyperpolarisation at sub-MIC without causing bacterial depolarisation. Conversely, sequences with membrane-insensitive conformations fail to shift the bacterial population towards hyperpolarised state. Structurally, the absence of disulfide bonds and the presence of membrane-induced dynamic helical structures characterize the hyperpolarising sequences.

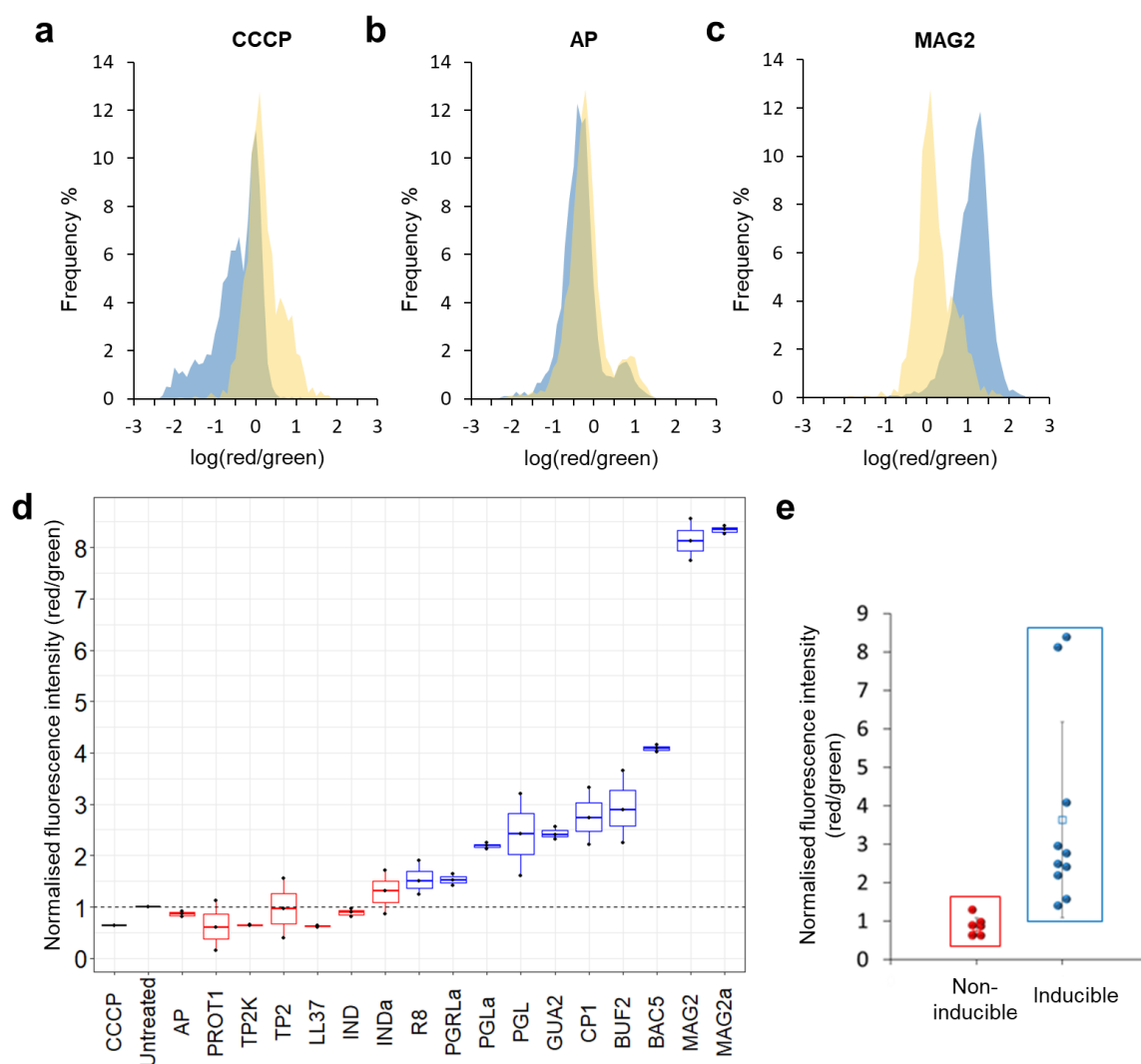


Figure 18: Flow cytometric membrane polarisation assay of AMPs in *E. coli* at 0.5 MIC. Histograms of (a) CCCP representing membrane depolarisation, (b) AP representing no effect on membrane potential, (c) MAG2a representing membrane hyperpolarisation. (d) Boxplot representing membrane polarisation change caused by AMPs. Ratio of red/green fluorescence were calculated using population mean fluorescence intensities for cells treated and normalised with untreated cells. If the ratio is below 1 correspond to depolarisation above 1 is hyperpolarisation. Data are based on 3 biological replicates. Boxplots show the median, first and third quartiles, with whiskers showing the minimum and maximum value. The dashed line represents no change. (e) Membrane polarisation data are shown in relation to the membrane-inducibility of the secondary structure.

We investigated whether these AMPs could hyperpolarise the membranes of Gram-positive organisms by testing with *Staphylococcus epidermidis*. MIC measurements for a selected panel of AMPs showed significantly higher values compared to those for *E. coli*. We conducted membrane potential assays at 0.5 MIC for AMPs demonstrating a notable antibiotic

effect against *S. epidermidis*. Under these conditions, these AMPs caused depolarisation of the membrane (Figure 19). Due to the relatively high MICs, the antibiotic concentrations used in this experiment were higher for *S. epidermidis* compared to *E. coli*. These findings suggest that AMP-induced hyperpolarisation at sub-MIC levels limited to Gram-negative bacteria like *E. coli*.

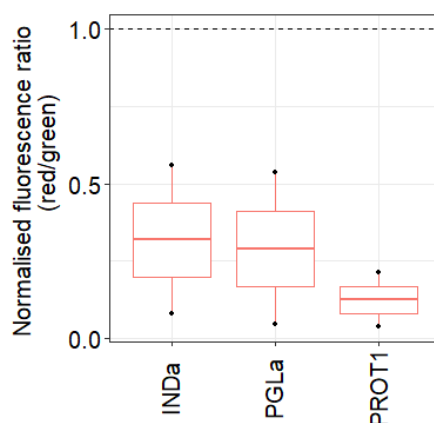


Figure 19: Membrane polarisation assay of AMPs in *S. epidermidis* at 0.5 MIC. The ratio below 1 correspond to depolarisation.

To evaluate whether AMPs could induce nonspecific currents through the membranes of eukaryotic cells, we measured the membrane potential of activated human peripheral lymphocytes using the patch-clamp technique in $I = 0$ current clamp mode was measured by Dr. Florina Zákány. We exposed human cells to PGLa and CP1. We also tested PGLb1 to suppress unwanted peptidase effects. The perfusion of high-concentration potassium solution (HK) was used as a positive control, which caused a reversible shift of the membrane potential close to 0 mV. This was followed by the application of PGLa, PGLb1, or CP1. Each peptide was dissolved in control bath solution at 0.5 MIC concentrations separately. In our measurements, we did not observe any significant changes in the resting membrane potential in response to long-term exposure to any of these peptides, as shown by representative traces (Figures 20a-c). Quantitative analysis of the data determined the relative changes in membrane potential due to exposure compared to the initial resting potential of the given cell ($\Delta E_m = E_{m_{\text{exposed}}} - E_{m_{\text{NR}}}$) (Figure 20d). PGLa, PGLb1, and CP1 induced negligible changes in membrane potential (-0.81 ± 0.77 , 0.49 ± 0.41 , and -0.17 ± 0.82 , respectively), suggesting that these compounds do not induce nonspecific conductance of ionic currents in eukaryotic cells.

We note that it is unlikely the AMPs internalized into the cytosol and organelles within the experimental timeframe, thereby ruling out potential intracellular effects.

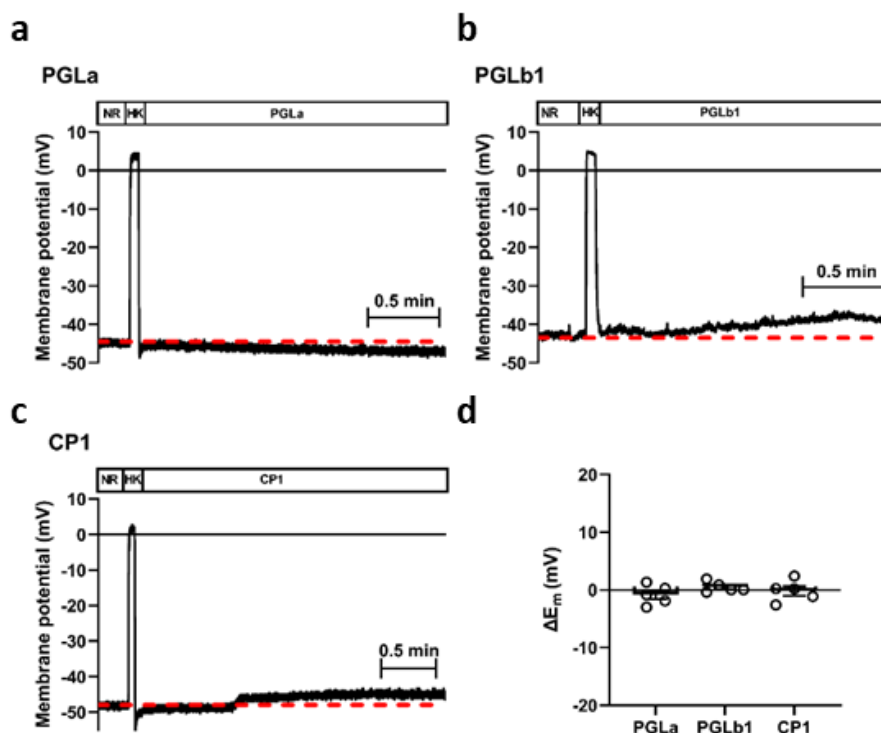


Figure 20: Patch-clamp membrane potential measurements for AMPs in human peripheral lymphocytes. Effects of PGLa, PGLb1, and CP1 exposition on the membrane potential using the patch-clamp technique in the current-clamp mode (a, b and c, respectively) at 0.5 MIC. (d) Column graph showing none of the examined materials caused biologically relevant changes in the resting membrane potential. Data are shown as mean \pm SEM (n=5), and dots represent values obtained from individual cells.

4.2.2. Concentration-dependent hyperpolarisation by AMPs

We proposed that AMP-induced hyperpolarisation is caused by the diffusion potential, driven by differences in relative ion permeabilities facilitated by peptide-mediated transmembrane ion transport. If the concentration of AMPs is sufficient for membrane binding and the formation of the required ionophoric structure, the relative ion permeabilities facilitated by the AMPs are expected to remain approximately constant. This hypothesis suggests that the diffusion potential remains stable when the AMP concentration is reduced, as long as it stays above the critical limit. On the other hand, the direct killing effect of AMPs relies on membrane rupture at or above the MIC, which is concentration dependent. As the MIC value approaches, the chances of nonselective pore formation and depolarisation increases. This effect can

compete with the diffusion potential, leading to reduced polarisation as the AMP concentration approaches the MIC. To test this hypothesis, we conducted measurements in the range of 0.25 – 0.75 MIC. An increase in hyperpolarisation with lower AMP concentrations was observed, supporting the presence of the diffusion potential as the underlying mechanism of the hyperpolarisation (Figure 21).

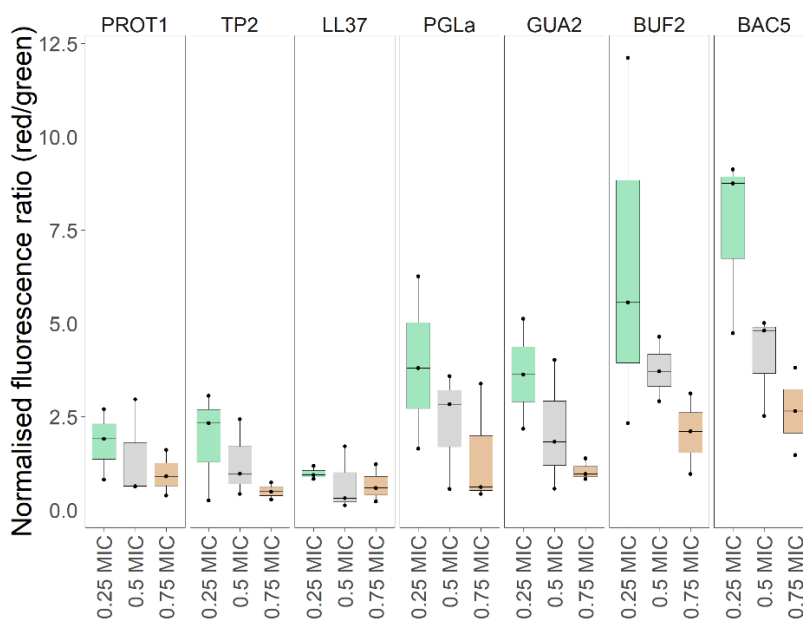


Figure 21: Flow cytometric membrane polarisation assay of AMPs in *E. coli* at different sub-MIC levels.

4.2.3. AMPs generate diffusion potential in LUVs

With the exception of AP, all AMPs induced alterations in bacterial electrophysiology at sub-inhibitory concentrations with many inducing hyperpolarisation. There were no significant cytosolic membrane damage or non-selective pore formation during the bacterial membrane hyperpolarisation. This raised the question of a generalised hyperpolarisation mechanism at sub-MIC, contrasting to the established membrane rupturing mechanism for cationic AMPs at lethal doses. As there are no internal cellular target is known for MAG2a, GUA2, R8, and PGLa, hyperpolarisation in bacterial membranes, without cytosolic damage or pore formation, suggests direct membrane-AMP interactions. Therefore, membrane polarisation experiment in LUV model with membrane potential dye Oxonol VI was conducted at 0.5 MIC (similar to section 4.1.6). Without ion gradient across the LUV membrane (100 mM NaCl outside/100 mM NaCl inside) impact of initial binding of the cationic regions of the

peptides to the negatively charged membrane caused mild increase in fluorescence level (Figure 22).

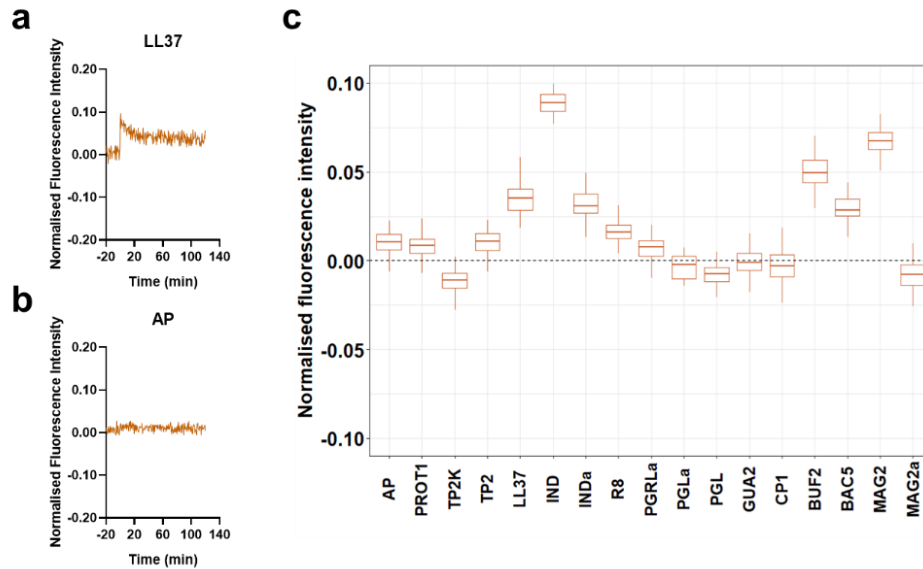


Figure 22: Static potential change induced by AMPs in the LUV model. Data are shown for (a) LL37 causing a mild increase and (b) AP causing little to no effect. (c) Boxplot presenting static potential change for all the AMPs. Boxplots show the median, first and third quartiles, with whiskers showing the minimum and maximum value. The dashed line represents no change.

When cation gradient K^+ (100 mM KCl outside)/ Na^+ (100 mM NaCl inside) was established, AMPs caused sequence dependent drop in fluorescence level suggesting generation of intravesicular negative potential via selective K^+ selectivity at sub-MIC concentrations. Membrane potential profiles of individual AMPs showed higher potential change for first few minutes, which then slowed down to reach a steady state for most of the AMPs (Figure 23a). diffusion potential analysis shows all AMPs except AP and CP1 showed some level of K^+ selective potential change (Figure 23b). PGLa generated highest membrane potential. These results correlate with biological measurements indicating diffusion potential plays a role in the membrane hyperpolarisation. In the same way, when anion gradient $H_2PO_4^-$ (100 mM NaH_2PO_4 outside)/ Cl^- (100 mM NaCl inside) was established, AMPs decreased the fluorescence due to the higher rate of transport of Cl^- compared to $H_2PO_4^-$ causing inside positive potential. diffusion potential analysis again showed except AP all the other AMPs caused potential change (Figure 23c).

Additionally, we carried out these measurements also with a NaCl inside and NaNO₃ outside gradient to eliminate potential osmotic stress due to the acid-base equilibrium of phosphate species. Changing the type of anion gradient to NO₃⁻ (100 mM NaNO₃ outside)/Cl⁻ (100 mM NaCl inside) caused similar decrease in fluorescence because of selectivity of Cl⁻ to NO₃⁻ but level of generated potential was lower compared to H₂PO₄⁻/Cl⁻ exchange (Figure 23d). This indicates that rate of movement of both ions involved might be important for the generation of the potential. Our findings suggest that the AMPs investigated induce diffusion potential in the LUV model in a sequence-dependent manner. The changes in fluorescence intensity indicate that AMPs generate diffusion potential through selective cross-membrane ion transport of K⁺ or Cl⁻, or both.

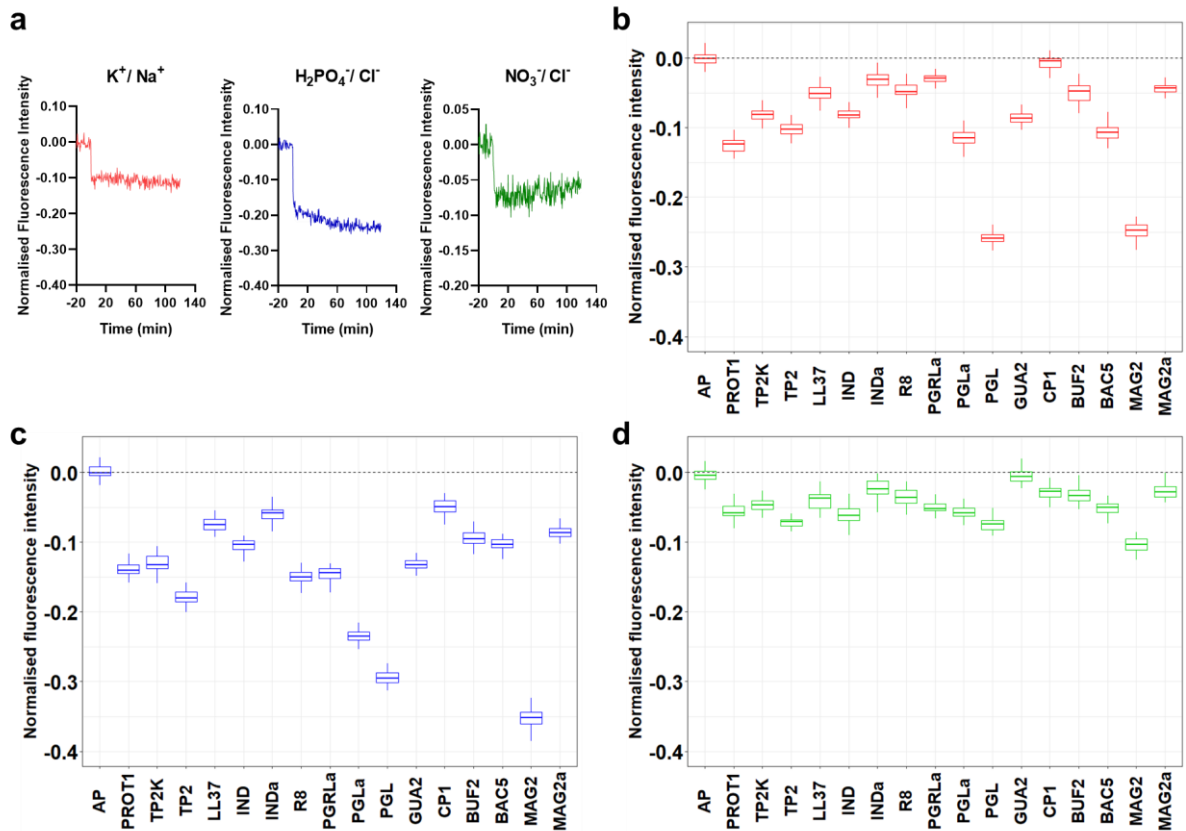


Figure 23: Membrane polarisation of AMPs in the LUV model. (a) diffusion potential change of PGLa in K⁺/Na⁺ [red], H₂PO₄⁻/ Cl⁻ [blue], NO₃⁻/ Cl⁻ [green] exchange. The negative change indicates a positive inside potential. Boxplots represent data for diffusion potential change for (b) K⁺/Na⁺ (c) H₂PO₄⁻/ Cl⁻, (d) NO₃⁻/ Cl⁻ exchange of all the AMPs. Boxplots show the median, first and third quartiles, with whiskers showing the minimum and maximum value. The dashed line represents no change.

These results support the notion that direct interactions between the membrane and AMPs at sub-inhibitory concentrations can influence diffusion potential across the lipid bilayer.

However, the structure induced by the membrane did not significantly contribute to diffusion potential generation in the LUV bilayer model. This observation strongly implies that components of the cell wall external to the cytoplasmic membrane modulate the hyperpolarisation effect in bacteria.

4.2.4. AMPs transport both cations and anions

To determine the rate and capability of transporting ions across the membrane of AMPs, NMR based time-dependent direct monitoring of Na^+ and H_2PO_4^- were done by detecting ^{23}Na and ^{31}P NMR signals in LUVs (similar to section 4.1.6). To monitor Na^+/K^+ exchange, ^{23}Na NMR was done on LUVs with 100 mM NaCl inside and 100 mM KCl outside. Dy^{3+} was used as NMR shift reagent to distinguish between inside and outside ^{23}Na NMR signal. All the AMPs showed time-dependent Na^+ transport at sub-inhibitory level (Figure 24). This experiment measures the slower rate determining step for Na^+/K^+ exchange. Similarly, to monitor $\text{H}_2\text{PO}_4^-/\text{Cl}^-$ exchange, ^{31}P NMR was done on LUVs with 100 mM NaH_2PO_4 inside and 100 mM NaCl outside. No shift reagent was needed in this case as the inside and outside ^{31}P could be distinguished clearly. All the AMPs showed time-dependent H_2PO_4^- transport at sub-inhibitory level AP, IND. This experiment measures the slower rate determining step for $\text{H}_2\text{PO}_4^-/\text{Cl}^-$ exchange. Cl^- transport was monitored by ^{35}Cl NMR on LUVs with 100 mM NaCl inside and 100 mM NaNO_3 outside. Co^{2+} was used as NMR shift reagent in this case. All the AMPs showed time-dependent Cl^- transport at sub-inhibitory level. The amount of Cl^- transport observed was significantly higher than the H_2PO_4^- transport for all the peptides as this experiment measures the faster rate determining step for $\text{Cl}^-/\text{NO}_3^-$ exchange.

Ion transport profiles of individual AMPs showed higher rate initial transport for first few minutes, which then slows down to reach a steady state. This might be because possible for several factors such as potential build up in the membrane over time, tighter interaction between the membrane and peptide, alteration of the lipid packing and ion competition for the binding site etc. Thus, analysis of the initial rate of transport analysis where all these factors have lesser role might be useful to analyse the capability for these peptides to transport ions. The initial ion transport rate for was calculated and represented for both Na^+/K^+ and $\text{H}_2\text{PO}_4^-/\text{Cl}^-$ exchange.

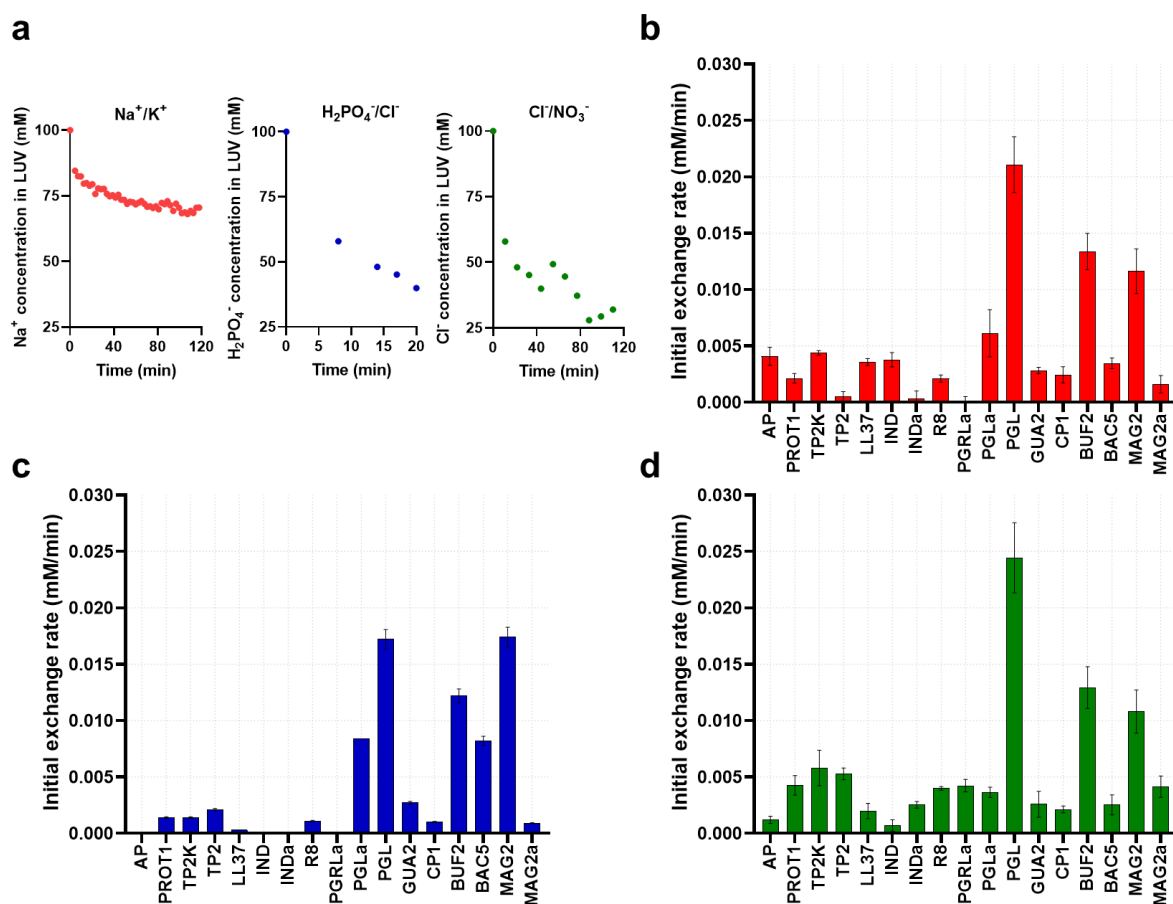


Figure 24: Ion transport measurements of AMPs in the LUV model. (a) Na⁺ transport [red], H₂PO₄⁻ transport [blue], Cl⁻ transport [green] of PGL in NMR. Bar plot represents the initial exchange rates observed for AMPs in the (b) Na⁺/K⁺, (c) H₂PO₄⁻/Cl⁻, (d) Cl⁻/NO₃⁻ gradient model. The ion concentration of Na⁺, H₂PO₄⁻, Cl⁻ were determined by ²³Na, ³¹P and ³⁵Cl NMR assay respectively.

4.3. Proposed mechanism of hyperpolarisation induced by AMPs

At higher concentration, AMPs typically show their effect by direct killing by membrane rupturing, but at lower sub-MIC levels, we have shown these cationic peptides induced changes membrane polarisation, majorly membrane hyperpolarisation. AMP sequences with higher structure inducibility in the presence of the membrane (as observed in CD results) showed high level of membrane potential in *E. coli* at sub-MIC. The findings suggest that a dynamic pre-equilibrium between the dissolved and membrane-bound peptides is necessary for selective behaviour.

Interestingly, lowering the hydrophobicity of PGLa by incorporating β-amino acids (PGLb1, PGLb2) showed improved diffusion potential, possibly by accelerating the on-off

dynamics of the membrane interaction. Ionophobic structures generally require structural flexibility to facilitate ion complexation, and the peptide flexibility may influence the rate of ion complexation and release processes, contributing to selective ion transport. PGLa, when immersed into the membrane at high potential, is less prone to trafficking between the solution phase and the membrane surface.¹⁷⁹ This observation may explain the cessation of ion transport seen in our NMR experiment after a certain period.

On the other hand, channel formation requires intimate membrane-peptide interaction, which may easily turn to membrane rupturing, emphasising the sensitivity and dynamic nature of this phenomenon. Our results strongly suggest that the environment-dependent structure is essential to cross the bacterial cell wall without damaging the membrane. The bacterial cell wall is a formidable barrier for antibacterial compounds due to the multiple lipophilic and negatively charged hydrophilic layers.¹⁸⁰ Crossing such a complex shield without a rupturing effect requires a flexible structure adapting to its actual environment. Thus, generating the diffusion potential at the inner cytosolic membrane is possible (Figure 25).

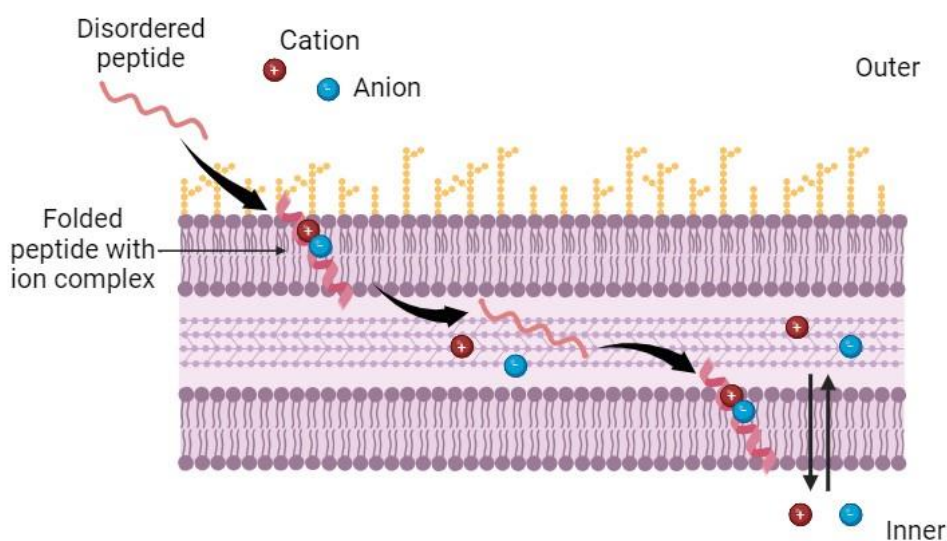


Figure 25: Representation of mechanism of membrane hyperpolarisation by AMPs at sub-MIC. Upon interacting with the membrane surface, AMPs fold and capture cations and anions, forming a neutral complex that can migrate into the membrane interior and diffuse across the pores of the bacterial cell wall. Once at the cytoplasmic membrane, diffusion potential generation becomes possible.

5. Conclusion

AMPs are potential candidates for targeting AMR as they attack bacteria in multiple mechanisms and have also been reported to reduce the resistance level in bacteria when used in combination with traditional antibiotics. In this study, we followed a rational design based on computer-assisted backbone homology and modified the secondary structure of the AMP called PGLa, resulting in two new peptidomimetics, PGLb1 and PGLb2. When administered at subinhibitory concentrations, PGLb1 and PGLb2 decreased the antibiotic resistance level of clinical isolates of *E. coli*, *K. pneumoniae*, and *S. flexneri* by up to 128 times. Furthermore, these compounds showed stability against human proteases and no toxicity in human red blood cells. These promising findings highlight the need for future chemical refinements to selectively enhance the potency of antibiotics against antibiotic-resistant bacteria. Our study has wider implications as it challenges the commonly held belief that AMPs cause membrane disruption. Instead, we found that PGLb1 and PGLb2 induce hyperpolarisation of the bacterial membrane at sub-MIC levels, by selectively transporting ions across the membrane, thereby inducing diffusion potential.

Again, we have shown that it is a common trait of AMPs to induce polarisation in membranes of gram-negative bacteria below the threshold of the MIC. This is accomplished through the differential rate of ion transport, specifically the selectivity of K^+ over Na^+ and Cl^- over $H_2PO_4^-$, resulting in the creation of diffusion potential. An exciting finding is that these peptides not only transport cations, but also demonstrate the ability to transport biologically important anions such as phosphate in bacteria through neutral complex formation. The lowered concentration prevented membrane rupture, while AMP-mediated selective ion transport facilitated shaping a diffusion potential. To describe the extent of the membrane polarisation as a function of the relative permeabilities and ion concentrations, the GHK model is an adequate framework, and in a future work, we plan to explore the exact quantitative relationship.

In summary, our study showcases the potential for rational design of novel peptidomimetic foldamer antimicrobials that induce hyperpolarisation of the bacterial membrane through a regulated biophysical mechanism, thus enhancing the susceptibility of multidrug resistant bacteria to existing antimicrobial agents. We also tried to shed light on the vague molecular mechanics of the sub-MIC activity of AMPs in general. Future research, involving a larger

variety of AMPs, can reveal the specific structural components to control ion transport and membrane polarisation.

6. Summary

1. A structure-based strategy was employed to modify PGLa, resulting in the synthesis of novel α/β -foldamer adjuvants (PGLb1, PGLb2, and PGLb3) by targeting different sites that interact with the bacterial membrane, aimed at improving antibiotic efficacy against resistant bacteria and enhancing resistance to human proteases.
2. Despite their weak intrinsic antibacterial activity, PGLb1 and PGLb2 demonstrated strong synergistic effects with Nalidixic acid across multiple *E. coli* isolates, in contrast to the primarily additive effect observed with PGLa.
3. In clinical isolates of nalidixic acid-resistant *E. coli*, *K. pneumoniae*, and *S. flexneri*, PGLb1 and PGLb2 significantly reduced antibiotic resistance at sub-MIC. These *in vitro* findings were validated *in vivo*, with PGLb1 notably enhancing the survival rate of *G. mellonella* larvae infected with nalidixic acid-resistant *E. coli*.
4. Flow cytometric analysis of *E. coli* revealed that PGLb1 and PGLb2 induce substantial and prolonged hyperpolarisation of the bacterial membrane, in contrast to the mild and transient effect observed with PGLa, providing insights into the mechanism behind the sub-MIC effect.
5. Studies using a LUV model demonstrated that PGLb1 and PGLb2 elicit the diffusion potential through time-dependent selective transport of cations (K^+ over Na^+) and anions (Cl^- over NO_3^-), providing deeper insights into the mechanisms underlying membrane hyperpolarisation.
6. An expanded study of 17 AMPs revealed that those with higher structure inducibility, as confirmed by CD measurements, caused membrane hyperpolarisation in *E. coli* at subinhibitory doses, indicating a common mechanism of action involving ion transport.
7. Membrane polarisation experiments with *S. epidermidis* demonstrated that AMP-induced hyperpolarisation is predominantly limited to Gram-negative bacteria, indicating a significant difference in response between Gram-positive and Gram-negative bacterial membranes.

8. Experiments conducted with AMP concentrations ranging from 0.25 to 0.75 MIC in *E. coli* demonstrated increasing membrane hyperpolarisation at lower concentrations, corroborating the diffusion potential mechanism.
9. Contrary to literature focusing mainly on cation (especially K^+) transport, our findings indicate that most AMPs can generate membrane potential by transporting both cations and anions, depending on their sequences, thereby maintaining a quasi-steady-state ion gradient.

Acknowledgement

First and foremost, I would like to express my sincere gratitude to my supervisor, Prof. Tamás A. Martinek, for his guidance and support throughout my doctoral studies. I am thankful for the opportunity to learn from his extensive expertise and knowledge in the field. His mentorship greatly helped me throughout my PhD research and writing of this thesis.

I would like to extend my gratitude to my co-supervisor, Dr. Hetényi Anasztázia for her regular support in the lab and as well as for her technical assistance and guidance with NMR experiments.

I would like to extend my gratitude to Prof. Csaba Pál and his lab members for conducting the biological experiments. Thank you to Dr. Balázs Jojart for conducting the molecular dynamics studies.

Similar thanks go to Dr. Livia Fülöp for the access of her lab to use DLS and other available instruments. I am thankful to Dr. Edit Csapó for CD spectrophotometer access.

Additionally, I would like to thank members of the Foldamer Lab, Dr. Attila Tököli, Dr. Éva Kovács-Bartus, Dr. Zsófia Hegedüs, Dr. Edit Wéber, Dr. Gábor Olajos, Dr. Brigitta Bodnár for their help in the lab.

I would like to express my gratitude to all my friends, Attila Tököli, Dániel Dancs, Zita Papp Ibolya, and Vencel Petrovicz for making my time in Hungary such a delightful journey filled with lifelong memories. From our cooking sessions to Christmas parties, and countless other amazing moments, you have all been truly wonderful colleagues and friends.

I extend my heartfelt gratitude to my partner Neha Sahu for her unwavering support throughout this journey. Her encouragement and understanding have been invaluable to me. I also thank her for teaching and helping me with R language to make figures.

Last but not the least, I would like to thank my parents and my sister for their kind support.

References

- 1 Antimicrobial resistance, <https://www.who.int/news-room/fact-sheets/detail/antimicrobial-resistance>, (accessed January 26, 2023).
- 2 E. M. Darby, E. Trampari, P. Siasat, M. S. Gaya, I. Alav, M. A. Webber and J. M. A. Blair, *Nat Rev Microbiol*, 2022, 1–16.
- 3 S. Ahmed, M. Z. Ahmed, S. Rafique, S. E. Almasoudi, M. Shah, N. A. C. Jalil and S. C. Ojha, *BioMed Research International*, 2023, **2023**, e5250040.
- 4 V. Bhandari and A. Suresh, *Frontiers in Pharmacology*.
- 5 S. J. Baker, D. J. Payne, R. Rappuoli and E. De Gregorio, *Proc Natl Acad Sci USA*, 2018, **115**, 12887–12895.
- 6 J. M. Benarroch and M. Asally, *Trends in Microbiology*, 2020, **28**, 304–314.
- 7 A. Muthaiyan, J. A. Silverman, R. K. Jayaswal and B. J. Wilkinson, *Antimicrobial Agents and Chemotherapy*, 2008, **52**, 980–990.
- 8 C. S. Lunde, S. R. Hartouni, J. W. Janc, M. Mammen, P. P. Humphrey and B. M. Benton, *Antimicrobial Agents and Chemotherapy*, 2009, **53**, 3375–3383.
- 9 B. Mishra, S. Reiling, D. Zarena and G. Wang, *Curr Opin Chem Biol*, 2017, **38**, 87–96.
- 10 D. L. Higgins, R. Chang, D. V. Debabov, J. Leung, T. Wu, K. M. Krause, E. Sandvik, J. M. Hubbard, K. Kaniga, D. E. Schmidt, Q. Gao, R. T. Cass, D. E. Karr, B. M. Benton and P. P. Humphrey, *Antimicrobial Agents and Chemotherapy*, 2005, **49**, 1127–1134.
- 11 W. F. Porto, L. Irazazabal, E. S. F. Alves, S. M. Ribeiro, C. O. Matos, Á. S. Pires, I. C. M. Fensterseifer, V. J. Miranda, E. F. Haney, V. Humblot, M. D. T. Torres, R. E. W. Hancock, L. M. Liao, A. Ladram, T. K. Lu, C. de la Fuente-Nunez and O. L. Franco, *Nature Communications*, 2018, **9**, 1490.
- 12 T.-W. Chang, S.-Y. Wei, S.-H. Wang, H.-M. Wei, Y.-J. Wang, C.-F. Wang, C. Chen and Y.-D. Liao, *PLOS ONE*, 2017, **12**, e0186442.
- 13 N. Mookherjee, M. A. Anderson, H. P. Haagsman and D. J. Davidson, *Nat Rev Drug Discov*, 2020, **19**, 311–332.
- 14 V. Lázár, A. Martins, R. Spohn, L. Daruka, G. Grézal, G. Fekete, M. Számel, P. K. Jangir, B. Kintses, B. Csörgő, Á. Nyerges, Á. Györkei, A. Kincses, A. Dér, F. R. Walter, M. A. Deli, E. Urbán, Z. Hegedűs, G. Olajos, O. Méhi, B. Bálint, I. Nagy, T. A. Martinek, B. Papp and C. Pál, *Nat Microbiol*, 2018, **3**, 718–731.
- 15 L. Lin, P. Nonejuie, J. Munguia, A. Hollands, J. Olson, Q. Dam, M. Kumaraswamy, H. Rivera, R. Corriden, M. Rohde, M. E. Hensler, M. D. Burkart, J. Pogliano, G. Sakoulas and V. Nizet, *EBioMedicine*, 2015, **2**, 690–698.
- 16 Q. Li, R. Cebrián, M. Montalbán-López, H. Ren, W. Wu and O. P. Kuipers, *Commun Biol*, 2021, **4**, 1–11.
- 17 K. R. Baker, B. Jana, A. M. Hansen, H. M. Nielsen, H. Franzyk and L. Guardabassi, *Frontiers in Cellular and Infection Microbiology*.
- 18 R. Spohn, L. Daruka, V. Lázár, A. Martins, F. Vidovics, G. Grézal, O. Méhi, B. Kintses, M. Számel, P. K. Jangir, B. Csörgő, Á. Györkei, Z. Bódi, A. Faragó, L. Bodai, I. Földesi, D. Kata, G. Maróti, B. Pap, R. Wirth, B. Papp and C. Pál, *Nat Commun*, 2019, **10**, 4538.
- 19 I. Nicolas, V. Bordeau, A. Bondon, M. Baudy-Floc'h and B. Felden, *PLOS Biology*, 2019, **17**, e3000337.
- 20 M. S. Zharkova, D. S. Orlov, O. Yu. Golubeva, O. B. Chakchir, I. E. Eliseev, T. M. Grinchuk and O. V. Shamova, *Front Cell Infect Microbiol*, , DOI:10.3389/fcimb.2019.00128.
- 21 D. Pletzer, S. C. Mansour and R. E. W. Hancock, *PLOS Pathogens*, 2018, **14**, e1007084.
- 22 M. Hartmann, M. Berditsch, J. Hawecker, M. F. Ardakani, D. Gerthsen and A. S. Ulrich, *Antimicrob Agents Chemother*, 2010, **54**, 3132–3142.
- 23 F. Parvez, J. Md. Alam, H. Dohra and M. Yamazaki, *Biochimica et Biophysica Acta (BBA) - Biomembranes*, 2018, **1860**, 2262–2271.
- 24 S. Guha, J. Ghimire, E. Wu and W. C. Wimley, *Chem. Rev.*, 2019, **119**, 6040–6085.
- 25 A. S. Vasilchenko and E. A. Rogozhin, *Front. Microbiol.*, , DOI:10.3389/fmicb.2019.01160.
- 26 B. H. Gan, J. Gaynord, S. M. Rowe, T. Deingruber and D. R. Spring, *Chem. Soc. Rev.*, 2021, **50**, 7820–7880.
- 27 C. S. Ho, C. T. H. Wong, T. T. Aung, R. Lakshminarayanan, J. S. Mehta, S. Rauz, A. McNally, B. Kintses, S. J. Peacock, C. de la Fuente-Nunez, R. E. W. Hancock and D. S. J. Ting, *The Lancet Microbe*, , DOI:10.1016/j.lanmic.2024.07.010.
- 28 J. Stautz, Y. Hellmich, M. F. Fuss, J. M. Silberberg, J. R. Devlin, R. B. Stockbridge and I. Hänelt, *J Mol Biol*, 2021, **433**, 166968.
- 29 P. C. Maloney, E. R. Kashket and T. H. Wilson, *Proceedings of the National Academy of Sciences*, 1974, **71**, 3896–3900.
- 30 H. Strahl and L. W. Hamoen, *Proceedings of the National Academy of Sciences*, 2010, **107**, 12281–12286.
- 31 R. J. Poole, *Annual Review of Plant Physiology*, 1978, **29**, 437–460.
- 32 S. Nakamura and T. Minamino, *Biomolecules*, 2019, **9**, 279.
- 33 T. A. Krulwich, G. Sachs and E. Padan, *Nat Rev Microbiol*, 2011, **9**, 330–343.

- 34 A. Prindle, J. Liu, M. Asally, S. Ly, J. Garcia-Ojalvo and G. M. Süel, *Nature*, 2015, **527**, 59–63.
- 35 C. R. MacNair and E. D. Brown, *mBio*, 2020, **11**, e01615-20.
- 36 R. E. W. Hancock and H.-G. Sahl, *Nat Biotechnol*, 2006, **24**, 1551–1557.
- 37 R. E. W. Hancock, E. F. Haney and E. E. Gill, *Nat Rev Immunol*, 2016, **16**, 321–334.
- 38 R. E. W. Hancock, M. A. Alford and E. F. Haney, *Nat Rev Microbiol*, 2021, **19**, 786–797.
- 39 S. V. Prasad, K. Fiedoruk, T. Daniluk, E. Piktel and R. Bucki, *Int J Mol Sci*, 2019, **21**, 104.
- 40 Y. Huan, Q. Kong, H. Mou and H. Yi, *Front Microbiol*, 2020, **11**, 582779.
- 41 G. Shi, X. Kang, F. Dong, Y. Liu, N. Zhu, Y. Hu, H. Xu, X. Lao and H. Zheng, *Nucleic Acids Res*, 2022, **50**, D488–D496.
- 42 G. Wang, X. Li and Z. Wang, *Nucleic Acids Research*, 2016, **44**, D1087–D1093.
- 43 F. Harris, S. R. Dennison and D. A. Phoenix, *Curr Protein Pept Sci*, 2009, **10**, 585–606.
- 44 S. Bakels, S. B. A. Porskamp and A. M. Rijs, *Angewandte Chemie International Edition*, 2019, **58**, 10537–10541.
- 45 M. S. Butler, K. A. Hansford, M. A. T. Blaskovich, R. Halai and M. A. Cooper, *J Antibiot*, 2014, **67**, 631–644.
- 46 M. Empting, , DOI:10.1039/9781788010153-00001.
- 47 R. E. W. Hancock and D. S. Chapple, *Antimicrobial Agents and Chemotherapy*, 1999, **43**, 1317–1323.
- 48 P. G. Arnison, M. J. Bibb, G. Bierbaum, A. A. Bowers, T. S. Bugni, G. Bulaj, J. A. Camarero, D. J. Campopiano, G. L. Challis, J. Clardy, P. D. Cotter, D. J. Craik, M. Dawson, E. Dittmann, S. Donadio, P. C. Dorrestein, K.-D. Entian, M. A. Fischbach, J. S. Garavelli, U. Göransson, C. W. Gruber, D. H. Haft, T. K. Hemscheidt, C. Hertweck, C. Hill, A. R. Horswill, M. Jaspars, W. L. Kelly, J. P. Klinman, O. P. Kuipers, A. J. Link, W. Liu, M. A. Marahiel, D. A. Mitchell, G. N. Moll, B. S. Moore, R. Müller, S. K. Nair, I. F. Nes, G. E. Norris, B. M. Olivera, H. Onaka, M. L. Patchett, J. Piel, M. J. T. Reaney, S. Rebuffat, R. P. Ross, H.-G. Sahl, E. W. Schmidt, M. E. Selsted, K. Severinov, B. Shen, K. Sivonen, L. Smith, T. Stein, R. D. Süßmuth, J. R. Tagg, G.-L. Tang, A. W. Truman, J. C. Vederas, C. T. Walsh, J. D. Walton, S. C. Wenzel, J. M. Willey and W. A. van der Donk, *Nat. Prod. Rep.*, 2012, **30**, 108–160.
- 49 A. Simons, K. Alhanout and R. E. Duval, *Microorganisms*, 2020, **8**, 639.
- 50 C. Shao, Y. Zhu, Z. Lai, P. Tan and A. Shan, *Future Medicinal Chemistry*, 2019, **11**, 2047–2050.
- 51 T. A. Martinek and F. Fuloep, *Chem. Soc. Rev.*, 2012, **41**, 687–702.
- 52 C. Cabrele, T. A. Martinek, O. Reiser and L. Berlicki, *J. Med. Chem.*, 2014, **57**, 9718–9739.
- 53 J. D. Sadowsky, J. K. Murray, Y. Tomita and S. H. Gellman, *ChemBioChem*, 2007, **8**, 903–916.
- 54 F. Fülöp, T. A. Martinek and G. K. Tóth, *Chem. Soc. Rev.*, 2006, **35**, 323–334.
- 55 W. S. Horne, L. M. Johnson, T. J. Ketas, P. J. Klasse, M. Lu, J. P. Moore and S. H. Gellman, *Proc Natl Acad Sci U S A*, 2009, **106**, 14751–14756.
- 56 M. R. Yeaman and N. Y. Yount, *Pharmacol Rev*, 2003, **55**, 27–55.
- 57 M. Paulmann, T. Arnold, D. Linke, S. Özdirekcan, A. Kopp, T. Gutschmann, H. Kalbacher, I. Wanke, V. J. Schuenemann, M. Habeck, J. Bürck, A. S. Ulrich and B. Schitteck, *Journal of Biological Chemistry*, 2012, **287**, 8434–8443.
- 58 M. Cytryńska and A. Zdybicka-Barabas, *Biomol Concepts*, 2015, **6**, 237–251.
- 59 A. Bellomio, P. A. Vincent, B. F. de Arcuri, R. N. Farias and R. D. Morero, *Journal of Bacteriology*, 2007, **189**, 4180–4186.
- 60 V. Teixeira, M. J. Feio and M. Bastos, *Progress in Lipid Research*, 2012, **51**, 149–177.
- 61 K. A. Brogden, *Nature Reviews Microbiology*, 2005, **3**, 238–250.
- 62 H. Jenssen, P. Hamill and R. E. W. Hancock, *Clinical Microbiology Reviews*, 2006, **19**, 491–511.
- 63 N. Mookherjee, M. A. Anderson, H. P. Haagsman and D. J. Davidson, *Nat Rev Drug Discov*, 2020, **19**, 311–332.
- 64 F. Wang, L. Qin, C. J. Pace, P. Wong, R. Malonis and J. Gao, *ChemBioChem*, 2012, **13**, 51–55.
- 65 J. M. David and A. K. Rajasekaran, *J Kidney Cancer VHL*, 2015, **2**, 15–24.
- 66 S. Huang, Y. Liu, W.-Q. Liu, P. Neubauer and J. Li, *Microorganisms*, 2021, **9**, 780.
- 67 Z. Su, J. J. Leitch, S. Sek and J. Lipkowski, *Langmuir*, 2021, **37**, 9613–9621.
- 68 R. Capone, M. Mustata, H. Jang, F. T. Arce, R. Nussinov and R. Lal, *Biophysical Journal*, 2010, **98**, 2644–2652.
- 69 H. Duclouhier, G. Molle and G. Spach, *Biophysical Journal*, 1989, **56**, 1017–1021.
- 70 T. Katsu, S. Nakao and S. Iwanaga, *Biological & Pharmaceutical Bulletin*, 1993, **16**, 178–181.
- 71 D. S. Orlov, T. Nguyen and R. I. Lehrer, *Journal of Microbiological Methods*, 2002, **49**, 325–328.
- 72 Y. Sokolov, T. Mirzabekov, D. W. Martin, R. I. Lehrer and B. L. Kagan, *Biochimica et Biophysica Acta (BBA) - Biomembranes*, 1999, **1420**, 23–29.
- 73 M. E. Mangoni, A. Aumelas, P. Charnet, C. Roumestand, L. Chiche, E. Despau, G. Grassy, B. Calas and A. Chavanieu, *FEBS Letters*, 1996, **383**, 93–98.
- 74 C. Ohmizo, M. Yata and T. Katsu, *Journal of Microbiological Methods*, 2004, **59**, 173–179.
- 75 B. L. Kagan, M. E. Selsted, T. Ganz and R. I. Lehrer, *Proc Natl Acad Sci U S A*, 1990, **87**, 210–214.
- 76 B. Zhang, X. Qin, M. Zhou, T. Tian, Y. Sun, S. Li, D. Xiao and X. Cai, *Cell Proliferation*, 2021, **54**, e13020.

- 77 N. H. O'Driscoll, O. Labovitiadi, T. P. T. Cushnie, K. H. Matthews, D. K. Mercer and A. J. Lamb, *Curr Microbiol*, 2013, **66**, 271–278.
- 78 J. A. Tincu, L. P. Menzel, R. Azimov, J. Sands, T. Hong, A. J. Waring, S. W. Taylor and R. I. Lehrer, *Journal of Biological Chemistry*, 2003, **278**, 13546–13553.
- 79 D. G. Lee, Y. Park, H. N. Kim, H. K. Kim, P. I. Kim, B. H. Choi and K.-S. Hahm, *Biochemical and Biophysical Research Communications*, 2002, **291**, 1006–1013.
- 80 M. Wenzel, C. H. R. Senges, J. Zhang, S. Suleman, M. Nguyen, P. Kumar, A. I. Chiriac, J. J. Stepanek, N. Raatschen, C. May, U. Krämer, H.-G. Sahl, S. K. Straus and J. E. Bandow, *ChemBioChem*, 2015, **16**, 1101–1108.
- 81 L. C. Salay, J. Procopio, E. Oliveira, C. R. Nakaie and S. Schreier, *FEBS Letters*, 2004, **565**, 171–175.
- 82 K. Hu, Y. Jiang, Y. Xie, H. Liu, R. Liu, Z. Zhao, R. Lai and L. Yang, *J. Phys. Chem. B*, 2015, **119**, 8553–8560.
- 83 X. Gong, L. A. Martin-Visscher, D. Nahirney, J. C. Vederas and M. Duszyk, *Biochimica et Biophysica Acta (BBA) - Biomembranes*, 2009, **1788**, 1797–1803.
- 84 G. Yue, D. Merlin, M. E. Selsted, W. I. Lencer, J. L. Madara and D. C. Eaton, *American Journal of Physiology-Gastrointestinal and Liver Physiology*, 2002, **282**, G757–G765.
- 85 H. j. Kim, S. s. Kim, M. h. Lee, B. j. Lee and P. d. Ryu, *The Journal of Peptide Research*, 2004, **64**, 151–158.
- 86 C.-F. Le, C.-M. Fang and S. D. Sekaran, *Antimicrob Agents Chemother*, 2017, **61**, e02340-16.
- 87 C. B. Park, K.-S. Yi, K. Matsuzaki, M. S. Kim and S. C. Kim, *Proceedings of the National Academy of Sciences*, 2000, **97**, 8245–8250.
- 88 C. Marchand, K. Krajewski, H.-F. Lee, S. Antony, A. A. Johnson, R. Amin, P. Roller, M. Kvaratskhelia and Y. Pommier, *Nucleic Acids Research*, 2006, **34**, 5157–5165.
- 89 A. Yonezawa, J. Kuwahara, N. Fujii and Y. Sugiura, *Biochemistry*, 1992, **31**, 2998–3004.
- 90 Y.-H. Ho, P. Shah, Y.-W. Chen and C.-S. Chen, *Molecular & Cellular Proteomics*, 2016, **15**, 1837–1847.
- 91 A. Patrzykat, C. L. Friedrich, L. Zhang, V. Mendoza and R. E. W. Hancock, *Antimicrobial Agents and Chemotherapy*, 2002, **46**, 605–614.
- 92 C. L. Friedrich, A. Rozek, A. Patrzykat and R. E. W. Hancock, *Journal of Biological Chemistry*, 2001, **276**, 24015–24022.
- 93 S. Cociancich, A. Dupont, G. Hegy, R. Lanot, F. Holder, C. Hetru, J. A. Hoffmann and P. Bulet, *Biochem J*, 1994, **300**, 567–575.
- 94 K. Miura, S. Ueno, K. Kamiya, J. Kobayashi, H. Matsuoka, K. Ando and Y. Chinzei, *Jzoo*, 1996, **13**, 111–117.
- 95 H. R. Chileveru, S. A. Lim, P. Chairatana, A. J. Wommack, I.-L. Chiang and E. M. Nolan, *Biochemistry*, 2015, **54**, 1767–1777.
- 96 J. H. Viel, A. H. Jaarsma and O. P. Kuipers, *ACS Synth. Biol.*, 2021, **10**, 600–608.
- 97 H. Brötz, G. Bierbaum, P. E. Reynolds and H.-G. Sahl, *European Journal of Biochemistry*, 1997, **246**, 193–199.
- 98 O. Chertov, D. F. Michiel, L. Xu, J. M. Wang, K. Tani, W. J. Murphy, D. L. Longo, D. D. Taub and J. J. Oppenheim, *Journal of Biological Chemistry*, 1996, **271**, 2935–2940.
- 99 M. G. Scott, E. Dullaghan, N. Mookherjee, N. Glavas, M. Waldbrook, A. Thompson, A. Wang, K. Lee, S. Doria, P. Hamill, J. J. Yu, Y. Li, O. Donini, M. M. Guarna, B. B. Finlay, J. R. North and R. E. W. Hancock, *Nat Biotechnol*, 2007, **25**, 465–472.
- 100 L. Madera and R. E. W. Hancock, *J Innate Immun*, 2012, **4**, 553–568.
- 101 K.-Y. (Grace) Choi and N. Mookherjee, *Front Immunol*, 2012, **3**, 149.
- 102 K. Brandenburg, L. Heinbockel, W. Correa and K. Lohner, *Biochimica et Biophysica Acta (BBA) - Biomembranes*, 2016, **1858**, 971–979.
- 103 H. Tsuzuki, T. Tani, H. Ueyama and M. Kodama, *Journal of Surgical Research*, 2001, **100**, 127–134.
- 104 Y. Ha, Y. Koo, S.-K. Park, G.-E. Kim, H. Bin Oh, H. Ryong Kim and J.-H. Kwon, *RSC Advances*, 2021, **11**, 32000–32011.
- 105 J. D. te Winkel, D. A. Gray, K. H. Seistrup, L. W. Hamoen and H. Strahl, *Front Cell Dev Biol*, 2016, **4**, 29.
- 106 Y. Takechi-Haraya, T. Ohgita, M. Kotani, H. Kono, C. Saito, H. Tamagaki-Asahina, K. Nishitsuji, K. Uchimura, T. Sato, R. Kawano, K. Sakai-Kato, K. Izutsu and H. Saito, *Sci Rep*, 2022, **12**, 4959.
- 107 K. W. Swana, R. Nagarajan and T. A. Camesano, *Microorganisms*, 2021, **9**, 1975.
- 108 J. Lin, J. Motylinski, A. J. Krauson, W. C. Wimley, P. C. Searson and K. Hristova, *Langmuir*, 2012, **28**, 6088–6096.
- 109 V. Lázár, G. Pal Singh, R. Spohn, I. Nagy, B. Horváth, M. Hrtyan, R. Busa-Fekete, B. Bogos, O. Méhi, B. Csörgö, G. Pósfai, G. Fekete, B. Szappanos, B. Kégl, B. Papp and C. Pál, *Molecular Systems Biology*, 2013, **9**, 700.
- 110 I. Greco, N. Molchanova, E. Holmedal, H. Jenssen, B. D. Hummel, J. L. Watts, J. Håkansson, P. R. Hansen and J. Svenson, *Sci Rep*, 2020, **10**, 13206.
- 111 D. D. Kang, J. Park and Y. Park, *Microbiology Spectrum*, 2022, **10**, e01494-22.
- 112 Q. Wang, Y. Xu and J. Hu, *RSC Advances*, 2022, **12**, 14485–14491.
- 113 M. L. Mangoni, A. M. McDermott and M. Zasloff, *Experimental Dermatology*, 2016, **25**, 167–173.

- 114 E. M. C. Chung, S. N. Dean, C. N. Propst, B. M. Bishop and M. L. van Hoek, *npj Biofilms Microbiomes*, 2017, **3**, 1–13.
- 115 J. Qi, R. Gao, C. Liu, B. Shan, F. Gao, J. He, M. Yuan, H. Xie, S. Jin and Y. Ma, *IDR*, 2019, **12**, 2865–2874.
- 116 H.-Y. Wang, J.-W. Cheng, H.-Y. Yu, L. Lin, Y.-H. Chih and Y.-P. Pan, *Acta Biomaterialia*, 2015, **25**, 150–161.
- 117 Y. Zhu, W. Hao, X. Wang, J. Ouyang, X. Deng, H. Yu and Y. Wang, *Medicinal Research Reviews*, 2022, **42**, 1377–1422.
- 118 J. Li, P. Fernández-Millán and E. Boix, *Current Topics in Medicinal Chemistry*, **20**, 1238–1263.
- 119 M. Song, Y. Liu, X. Huang, S. Ding, Y. Wang, J. Shen and K. Zhu, *Nat Microbiol*, 2020, **5**, 1040–1050.
- 120 R. P. Darveau, M. D. Cunningham, C. L. Seachord, L. Cassiano-Clough, W. L. Cosand, J. Blake and C. S. Watkins, *Antimicrobial Agents and Chemotherapy*, 1991, **35**, 1153–1159.
- 121 A. Giacometti, O. Cirioni, M. S. Del Prete, A. M. Paggi, M. M. D’Errico and G. Scalise, *Peptides*, 2000, **21**, 1155–1160.
- 122 K. Hilpert, B. McLeod, J. Yu, M. R. Elliott, M. Rautenbach, S. Ruden, J. Bürck, C. Muhle-Goll, A. S. Ulrich, S. Keller and R. E. W. Hancock, *Antimicrobial Agents and Chemotherapy*, 2010, **54**, 4480–4483.
- 123 H. S. Sader, K. A. Fedler, R. P. Rennie, S. Stevens and R. N. Jones, *Antimicrobial Agents and Chemotherapy*, 2004, **48**, 3112–3118.
- 124 D. D. Boehr, K. Draker, K. Koteva, M. Bains, R. E. Hancock and G. D. Wright, *Chemistry & Biology*, 2003, **10**, 189–196.
- 125 V. Sass, T. Schneider, M. Wilmes, C. Körner, A. Tossi, N. Novikova, O. Shamova and H.-G. Sahl, *Infection and Immunity*, 2010, **78**, 2793–2800.
- 126 E. de Leeuw, C. Li, P. Zeng, C. Li, M. D. Buin, W.-Y. Lu, E. Breukink and W. Lu, *FEBS Letters*, 2010, **584**, 1543–1548.
- 127 H. Ulvatne, S. Karoliussen, T. Stiberg, Ø. Rekdal and J. S. Svendsen, *Journal of Antimicrobial Chemotherapy*, 2001, **48**, 203–208.
- 128 A.-K. Pöppel, H. Vogel, J. Wiesner and A. Vilcinskas, *Antimicrobial Agents and Chemotherapy*, 2015, **59**, 2508–2514.
- 129 M. Rahnamaeian, M. Cytryńska, A. Zdybicka-Barabas, K. Dobszlaff, J. Wiesner, R. M. Twyman, T. Zuchner, B. M. Sadd, R. R. Regoes, P. Schmid-Hempel and A. Vilcinskas, *Proceedings of the Royal Society B: Biological Sciences*, 2015, **282**, 20150293.
- 130 P. K. Singh, B. F. Tack, P. B. McCray and M. J. Welsh, *Am J Physiol Lung Cell Mol Physiol*, 2000, **279**, L799–805.
- 131 M. D. T. Torres, M. C. R. Melo, L. Flowers, O. Crescenzi, E. Notomista and C. de la Fuente-Nunez, *Nat Biomed Eng*, 2022, **6**, 67–75.
- 132 J. Zerweck, E. Strandberg, O. Kukhareenko, J. Reichert, J. Bürck, P. Wadhvani and A. S. Ulrich, *Sci Rep*, 2017, **7**, 13153.
- 133 E. Han and H. Lee, *RSC Adv.*, 2014, **5**, 2047–2055.
- 134 M. Cassone and L. Otvos Jr, *Expert Review of Anti-infective Therapy*, 2010, **8**, 703–716.
- 135 T. Lüders, G. A. Birkemo, G. Fimland, J. Nissen-Meyer and I. F. Nes, *Appl Environ Microbiol*, 2003, **69**, 1797–1799.
- 136 S. N. Dean, B. M. Bishop and M. L. van Hoek, *BMC Microbiology*, 2011, **11**, 114.
- 137 E. Mataraci and S. Dosler, *Antimicrob Agents Chemother*, 2012, **56**, 6366–6371.
- 138 N. de J. Pimentel-Filho, M. C. de F. Martins, G. B. Nogueira, H. C. Mantovani and M. C. D. Vanetti, *International Journal of Food Microbiology*, 2014, **190**, 1–8.
- 139 J. M. Shin, I. Ateia, J. R. Paulus, H. Liu, J. C. Fenno, A. H. Rickard and Y. L. Kapila, *Frontiers in Microbiology*.
- 140 A. Algburi, S. Zehm, V. Netrebov, A. B. Bren, V. Chistyakov and M. L. Chikindas, *Probiotics & Antimicro. Prot.*, 2017, **9**, 81–90.
- 141 L. A. Vega and M. G. Caparon, *Mol Microbiol*, 2012, **85**, 1119–1132.
- 142 L. Fernández, H. Jenssen, M. Bains, I. Wiegand, W. J. Gooderham and R. E. W. Hancock, *Antimicrobial Agents and Chemotherapy*, 2012, **56**, 6212–6222.
- 143 P. M. Schlievert, L. C. Case, K. A. Nemeth, C. C. Davis, Y. Sun, W. Qin, F. Wang, A. J. Brosnahan, J. A. Mleziva, M. L. Peterson and B. E. Jones, *Biochemistry*, 2007, **46**, 14349–14358.
- 144 J. Li, W. Wang, S. X. Xu, N. A. Magarvey and J. K. McCormick, *Proceedings of the National Academy of Sciences*, 2011, **108**, 3360–3365.
- 145 J.-L. Yu and L. Guo, *J. Proteome Res.*, 2011, **10**, 2992–3002.
- 146 W.-C. Tsai, Z.-J. Zhuang, C.-Y. Lin and W.-J. Chen, *Journal of Applied Microbiology*, 2016, **121**, 952–965.
- 147 D. H. Limoli, A. B. Rockel, K. M. Host, A. Jha, B. T. Kopp, T. Hollis and D. J. Wozniak, *PLOS Pathogens*, 2014, **10**, e1004083.
- 148 W. Li, N. M. O’Brien-Simpson, J. Tailhades, N. Pantarat, R. M. Dawson, L. Otvos, E. C. Reynolds, F. Separovic, M. A. Hossain and J. D. Wade, *Chemistry & Biology*, 2015, **22**, 1250–1258.

- 149 T.-S. Tseng, S.-H. Wang, T.-W. Chang, H.-M. Wei, Y.-J. Wang, K.-C. Tsai, Y.-D. Liao and C. Chen, *PLOS ONE*, 2016, **11**, e0164597.
- 150 N. Y. Yount, S. E. Cohen, D. Kupferwasser, A. J. Waring, P. Ruchala, S. Sharma, K. Wasserman, C.-L. Jung and M. R. Yeaman, *PLOS ONE*, 2011, **6**, e26727.
- 151 K. Thevissen, A. Ghazi, G. W. De Samblanx, C. Brownlee, R. W. Osborn and W. F. Broekaert, *Journal of Biological Chemistry*, 1996, **271**, 15018–15025.
- 152 Q. Wang, Y. Xu, M. Dong, B. Hang, Y. Sun, L. Wang, Y. Wang, J. Hu and W. Zhang, *Molecules*, 2018, **23**, 2026.
- 153 S. J. Shirbin, I. Insua, J. A. Holden, J. C. Lenzo, E. C. Reynolds, N. M. O'Brien-Simpson and G. G. Qiao, *Advanced Healthcare Materials*, 2018, **7**, 1800627.
- 154 J. C. M. Stewart, *Analytical Biochemistry*, 1980, **104**, 10–14.
- 155 M. Mahlapuu, C. Björn and J. Ekblom, *Critical Reviews in Biotechnology*, 2020, **40**, 978–992.
- 156 S. B. Rezende, K. G. N. Oshiro, N. G. O. Júnior, O. L. Franco and M. H. Cardoso, *Chem. Commun.*, 2021, **57**, 11578–11590.
- 157 X. Chen, X. Wu and S. Wang, *npj Sci Food*, 2022, **6**, 57.
- 158 Z. Szűcs, I. Bereczki, F. Fenyvesi, P. Herczegh, E. Ostorházi and A. Borbás, *Sci Rep*, 2022, **12**, 20921.
- 159 E. A. Porter, B. Weisblum and S. H. Gellman, *J. Am. Chem. Soc.*, 2002, **124**, 7324–7330.
- 160 E. Glattard, E. S. Salnikov, C. Aisenbrey and B. Bechinger, *Biophysical Chemistry*, 2016, **210**, 35–44.
- 161 L. M. Johnson and S. H. Gellman, *Methods Enzymol.*, 2013, **523**, 407–429.
- 162 W. S. Horne and S. H. Gellman, *Accounts of chemical research*, 2008, **41**, 1399.
- 163 E. A. Porter, X. Wang, H.-S. Lee, B. Weisblum and S. H. Gellman, *Nature*, 2000, **404**, 565–565.
- 164 G. N. Tew, R. W. Scott, M. L. Klein and W. F. DeGrado, *Acc. Chem. Res.*, 2010, **43**, 30–39.
- 165 J. Sarkis and V. Vié, *Frontiers in Bioengineering and Biotechnology*.
- 166 L. S., The problem of synergism and antagonism of combined drugs, <https://pubmed.ncbi.nlm.nih.gov/13081480/>, (accessed September 21, 2020).
- 167 M. F. Pereira, C. C. Rossi, G. C. da Silva, J. N. Rosa and D. M. S. Bazzolli, *Pathogens and Disease*, 2020, **78**, ftaa056.
- 168 H.-J. Apell and B. Bersch, *Biochimica et Biophysica Acta (BBA) - Biomembranes*, 1987, **903**, 480–494.
- 169 H. Tamagawa, *J Biol Phys*, 2019, **45**, 13–30.
- 170 X.-X. Zhou, W.-F. Li and Y.-J. Pan, *Journal of Peptide Science*, 2008, **14**, 697–707.
- 171 J. P. Tam, C. Wu and J.-L. Yang, *European Journal of Biochemistry*, 2000, **267**, 3289–3300.
- 172 F. Vernen, P. J. Harvey, S. A. Dias, A. S. Veiga, Y.-H. Huang, D. J. Craik, N. Lawrence and S. Troeira Henriques, *International Journal of Molecular Sciences*, 2019, **20**, 4184.
- 173 J. Turner, Y. Cho, N.-N. Dinh, A. J. Waring and R. I. Lehrer, *Antimicrobial Agents and Chemotherapy*, 1998, **42**, 2206–2214.
- 174 A. S. Ladokhin, M. E. Selsted and S. H. White, *Biochemistry*, 1999, **38**, 12313–12319.
- 175 C. Loose, K. Jensen, I. Rigoutsos and G. Stephanopoulos, *Nature*, 2006, **443**, 867–869.
- 176 E. Strandberg, P. Wadhvani, P. Tremouilhac, U. H. N. Dürr and A. S. Ulrich, *Biophys J*, 2006, **90**, 1676–1686.
- 177 C. Avitabile, L. D. D'Andrea and A. Romanelli, *Sci Rep*, 2014, **4**, 4293.
- 178 T. Niidome, H. Mihara, M. Oka, T. Hayashi, T. S. Kazutoshiyoshida and H. Aoyagi, *The Journal of Peptide Research*, 1998, **51**, 337–345.
- 179 L. J. Németh, T. A. Martinek and B. Jójárt, *J. Chem. Inf. Model.*, 2022, **62**, 4963–4969.
- 180 K. Lewis, *Cell*, 2020, **181**, 29–45.

Appendix